 doi:10.20944/preprints202208.0366.v1

A review of mechanics-based mesoscopic membrane remodelling methods: Capturing both the physics and the chemical diversity

Gaurav Kumar,[1] Satya Chaithanya Duggisetty,[1] and Anand Srivastava[1, a)]

Molecular Biophysics Unit, Indian Institute of Science Bangalore, C. V. Raman Road, Bangalore, Karnataka 560012, India

[a)]Electronic mail: anand@iisc.ac.in

 doi:10.20944/preprints202208.0366.v1

ABSTRACT

Specialized classes of proteins, working together in a tightly orchestrated manner, induce and maintain highly curved cellular and organelles membrane morphology. Due to the various experimental constraints, including the resolution limits of imaging techniques, it is non-trivial to accurately elucidate interactions among the various components involved in membrane deformation. The spatial and temporal scales of the systems also make it formidable to investigate them using simulations with molecular details. Interestingly, mechanics-based mesoscopic models have been used with great success in recapitulating the membrane deformations observed in experiments. In this review, we collate together and discuss the various mechanics based mesoscopic models for protein-mediated membrane deformation studies. In particular, we provide an elaborate description of a mesoscopic model where the membrane is modeled as a triangulated sheet and proteins are represented as either nematics or filaments. This representation allows us to explore the various aspects of protein-protein and protein-membrane interactions as well as examine the underlying mechanistic pathways for emergent behavior such as curvature-mediated protein localization and membrane deformation. We also put forward current efforts in the field towards back-mapping these mesoscopic models to finer-grained particle based models - a framework that could be used to explore how molecular interactions propagate to physical scales and vice-versa. We end the review with an integrative-modeling based road map where experimental imaging micrograph and biochemical data are combined with mesoscopic and molecular simulations methods in a theoretically consistent manner to faithfully recapitulate the multiple length and time scales in the membrane remodeling processes.

KEYWORDS

Curvature proteins, Membrane Remodelling, Protein-protein interactions, Mesoscopic Modeling, Backmapping and molecular reconstruction

 doi:10.20944/preprints202208.0366.v1

I. INTRODUCTION

Biological membranes undergo dramatic changes in curvature and morphology during processes such as endocytosis, immune response, vesicular transport, and cell division. Membrane remodeling is a very dynamic process with a steady state distribution of membrane proteins and lipids across the cellular compartments[1]. This homeostatic distribution is regulated by a fine balance between competing dynamic processes such as endocytosis, recycling and exocytosis - processes modulated by membrane budding, scission and fusion of transport carriers. The molecular machines in these extremely sophisticated "biological circuitry" encrypt and process complex set of information in a precise manner across multiple length and time scales ranging from atom-level interactions and formation of molecular and macromolecular complexes to vesicular transport. Clathrin-mediated endocytosis (CME) is quintessential example where more than 50 different proteins are known to work together in a highly coordinated manner across time and space for successful completion of the process[2,3]. Some other very well known examples include endoplasmic reticulum (ER) and Golgi trafficking and their dynamics. For example, it has been long established that Golgi complex trafficking and dynamics are regulated by association of several proteins such as microtubules, ankyrin, spectrin, dynein, kinesin and myosin[4]. The highly tubular network of membrane structure in ER is supported and maintained by numerous proteins including the well-known ER-shaping proteins such as atlastin, lunapark, and reticulons[5]. With their presence in more than 750 proteins, the numerous sub-families of BIN-Amphiphysin-Rvs (BAR) domain containing proteins continuously shape and reshape membrane across organelles and mediate cellular and sub-cellular events such as actin assembly, sorting, endocytic trafficking and vesicular transport[6,7].

Though the remodeling processes in vesicular transport pathways are mediated by multiple curvature proteins interacting in concert with each other, this aspect has not been studied very much in reconstitution experiments[3,8–13]. This is primarily because of the spatial and temporal resolution limits of even the most advanced high-resolution microscopy/imaging techniques which makes it extremely difficult to probe the interplay (in real time) among the multiple kinds of proteins leading to membrane deformation and trafficking. As such, decoupling the role of individual components in the intricate remodeling machinery is one

 doi:10.20944/preprints202208.0366.v1

of the biggest challenges towards mechanistic understanding of the underlying processes. Elucidation of the molecular design-level features leading to the tightly regulated deformation and vesicular transport can help us gain fundamental insights into how these complex machineries have matured over evolutionary timescales and how they function[14]. Newer and deeper insights, at multiple scales ranging from molecular interactions to physical scales, can be obtained by following what is now called as "integrative modeling" approach[15–17]. Here, (mostly low-resolution and ensemble averaged) information from various kinds of experiments are integrated with multiscale simulation methods using theoretically well-grounded optimization frameworks such as Bayesian inference, genetic algorithms and machine learning methods[18–22]. Since the bounds are set by experimental constraints, the integrative approach could be used to gain additional insights into the mechanisms leading to the complex membrane remodeling processes.

Ideally, high-resolution all-atom molecular dynamics (AAMD) simulation is the most preferred method to faithfully recapitulate the intricacies of these processes[23–26] but infeasible due to the computational costs of the larger systems under consideration. For emergent process such as ones described above, highly coarse-grained molecular dynamics (CGMD) models have provided important insights into the pathway leading to large deformations[27–29]. However, even CGMD simulations can be computationally prohibitive since some of the processes takes places in seconds and minutes timescales[30–32]. Continuum mechanics based mesoscopic modeling can be used to simulate proteins-induced membrane curvatures and probe the underlying physical forces driving these processes on large time and length scales. In this paper, we review the various continuum-scale mesoscopic models available in the literature. Additionally, in our efforts to connect multiple length and times scales by a combination of continuum-level mesoscopic modeling and finer-grained molecular simulations, we will also highlight the need to reconstruct the continuum representation into finer-grained models with molecular details such that atomistic and molecular driving forces underlying these processes could also be explored with minimal computational costs. In a truly integrative modeling approach, the road map towards reconstruction of detailed molecular models from continuum representation should incorporate experimental inputs both at the imaging level as well as at structural and biochemical scales.

Our review is organized as follows. In the second section, we provide a historical perspec-

 doi:10.20944/preprints202208.0366.v1

tive on the analytical/computational approaches to model membrane deformation, which starts with the discussion from the seminal work of Canham and Helfrich and to the most recent advances in mesoscopic modeling of protein-induced membrane remodeling. In the third section, we particularly focus on a popular mesoscopic model where protein is represented as either a nematic or filament and membrane is treated as a triangulated surface. We will show that this is a very rich Physics-based model with the capability to rigorously study the role of lipid-protein and protein-protein interactions leading to large scale deformations. The model also lends itself to molecular reconstruction in a very amenable manner with minimal ambiguity. We discuss the various possible applications of the aforesaid mentioned model in the fourth section of our review article. We also include a section on what we think are the challenges and opportunities in the field of theoretical and computational biophysics of membrane remodelling. Among other things, here we discuss the current status and challenges of molecular reconstruction from mesoscopic representation and challenges in modeling deformation due to the active filamentous mesh work within the cell.

II. MESOSCOPIC MODELLING WITH CONTINUUM REPRESENTATION - A BRIEF SURVEY OF EXISTING METHODS

The earliest analytical models of membrane deformation were proposed by Canham and Helfrich in the 1970s[33,34]. Also, some of the early analytical papers written by Thomas Fischer[35–39], Udo Seifert[40–42] and Reinhard Lipowsky[43–45] have set the stage for deeper theoretical and computational studies in large scale membrane deformation. Also, several numerical simulation methods such as dissipative particle dynamics (DPD), Brownian dynamics (BD) and molecular dynamics (MD) have been used to study protein-mediated membrane remodelling at mesoscopic scales[23,27–29,46–56]. In this review, we do not discuss mesoscopic models for membrane remodeling where the lipids and proteins are represented as discrete particles and the the Hamiltonian (force-field) is solved with the evolution methods such as DPD, BD or MD. We list a few references here that can be used as starting points to explore the literature in the area of particle-based CG simulations in the membrane remodeling[57–61]. We also refer the readers to a few recent excellent reviews that focus on multiscale simulations approaches to membrane remodeling[62–64]. In this review, we limit our discussions

Preprints (www.preprints.org) | NOT PEER-REVIEWED | Posted: 22 August 2022 doi:10.20944/preprints202208.0366.v1

to mesocopic models with field-based approaches where the representation of membrane is continuum in nature and the Hamiltonian is guided by the Physics of membrane deformation rather than molecular scale force-field functions as in particle-based CG simulations. Also, there are several instances of the membrane curvature that are maintained away from the equilibrium and constantly undergo topological changes in terms of fusion and fission reactions such as those seen in Golgi complex and Endoplasmic Reticulum dynamics[4,5,65–68], which we do not elaborate upon in this review and have limited our scope to systems with no genus nor holes – most of the examples discussed here are for closed surfaces where the total Gaussian curvature is a positive constant.

One of the main approach of analytically determining membrane equilibrium shape is to cast it as an energy-minimizing functional variation problem subject to problem-specific geometric constraints. In most cases, the membrane is modeled as a discretized closed surface and proteins are either implicitly represented or introduced as inclusions[69–72]. We refer to some recent papers from Hiroshi Noguchi and co-workers[73–75] and Thomas Weikl and co-workers[76–79]. Noguchi et al. use coarse-grained meshless membrane simulations[73,80] where the proteins are modelled as banana-shaped chains of beads and the membrane is modelled as a two-dimensional sheet of beads. They show that tubulation depends on the curvatures of both inclusions and proteins. When both inclusion and proteins curvatures have the same sign, tubulation is promoted otherwise percolated-network is formed. When equal amounts of the two opposite inclusions are added, their effects cancel each other and in this case tubulation is slowly accelerated. Another elegant and theoretically well grounded method called second generation elastic membrane (EM2) model from Gregory Voth group[81,82] is worth mentioning here. EM2 is based on the seminal smooth particle applied Mmchanics (SPAM) framework developed by W.G. Hoover[83,84]. Though the EM2 model is largely based on field theory approach where membrane and solvents are considered as quasi particles, it can be more naturally linked to particle based dynamics if one wants to map the outcomes to high-resolution particle-based models. Since EM2 is characterized by protein density and lipid composition that can exchange with nearby particles, a large scale membrane topological changes and lipid domain formation can be studied with this model. However, it could be studied only for two scenarios of protein density that are given by spontaneous curvature of the protein when binding on to the membranes with 100 percent coverage and

Preprints (www.preprints.org) | NOT PEER-REVIEWED | Posted: 22 August 2022 doi:10.20944/preprints202208.0366.v1

zero percent coverage. To address this limitation, EM2 was recently extended as Mesoscopic Membrane with Proteins (MesM-P) in Voth group[85] where more than one type of membrane and solvent quasi particles can be incorporated. The method is available as a freeware package on LAMMPS and this model can be used to study membrane with different protein densities.

Another method known as dynamically triangulated surface (DTS), and the one that we are going to discuss in great detail in this review, was first used in the context of polymerized membranes[86]. This framework was extended by Baumgartner and Ho[87,88] to study fluid membranes and further improved and popularized by extensive membrane biophysics work from the likes of Lipowsky, Kroll and Gompper[43,44,89–92]. The introduction of nematics to model proteins on the triangulated surface framework has its first implementations in the groups of John Ipsen and P.B. Sunil Kumar where they used an augmented Helfrich-based Hamiltonian to model the protein-induced membrane deformation[93–96]. Anirban Sain laboratory at IIT, Bombay[97–99] and Ravi Radhakrishnan laboratory at University of Pennsylvania[100,101] have also used DTS method extensively. We find that among the existing continuum-scale mesoscopic model, this model is most amenable to accurate back mapping reconstruction to molecular details. In this model, the protein is modeled as a nematic field adhering to a deformable fluid membrane surface and the membrane is represented as triangulated sheet. The local orientation of the nematic field is denoted by the unit vector which lies in the local tangent plane of the membrane and is free to rotate in this plane. Protein-membrane interactions are modelled as anisotropic spontaneous curvatures of the membrane, in the vicinity of the nematics. Protein-protein interactions are modelled by the splay and bend terms of the Frank's free energy for nematic liquid crystals[102]. In the following segments, we discuss the details of the nematics based membrane deformation model.

III. DYNAMICALLY TRIANGULATED SURFACE (DTS) METHOD FOR MESOSCOPIC MEMBRANE REMODELING

A. Hamiltonian of the DTS model

In the DTS method, we model the membrane as two dimensional quasi-elastic sheet and represent it as a triangulated sheet. For example, to model a vesicle, the continuum surface

Preprints (www.preprints.org) | NOT PEER-REVIEWED | Posted: 22 August 2022 doi:10.20944/preprints202208.0366.v1

of spherical topology is replaced by a mesh of $N_T = 2(N_v - 2)$ triangles with N_v vertices connected by $N_E = 3(N_v - 2)$ edges. A triangulated sphere forms a polyhedron that obeys Euler characteristic, which is defined based on the number of vertices. Euler characteristic is a topological invariant ($\chi = N_v - N_E + N_T{=}2$) – a number that describe the topological space that does not vary irrespective of deformation profile. Here, a bead is assigned with unit diameter (a) and is fixed on every vertex with a maximum tether length of $\sqrt{3}a$ between two neighboring beads. Though this prevents the vertices from collapsing into each other, we also put a penalty on the angle between the normal of the two triangulated plane with a common edge. With this requirement for the continuum analytical modeling where the total Gaussian curvature is a constant, a strict self-avoidance of the surface is guaranteed. The bending elastic energy of the membrane is formulated in terms of local curvature using the classical Helfrich theory[34] and is written as:.

$$E_1 = \frac{\kappa}{2}\int (2H)^2 dA + \kappa_G \int G\ dA \tag{1}$$

where H and G are the local mean curvature and Gaussian curvature of membrane, respectively The mean and Gaussian curvatures are expressed as $H = (c_1 + c_2)/2$ and $G = c_1 c_2$ where c_1 and c_2 are the local principal curvatures on the membrane surface along the orthogonal principal directions $\hat{t}_1$ and $\hat{t}_2$ (see Fig. 1). κ represents the mean curvature bending rigidity of the membrane and κ_G is the Gaussian rigidity of the membrane. For the closed vesicle, the total Gaussian curvature of the membrane is constant as no total effective topological change is tolerated in continuum modeling.

In the DTS method, proteins are modeled as nematics[93–96] and recently the model has been enhanced to incorporate filaments as inclusions[98,99]. These nematic inclusions can move from vertex to vertex and are free to rotate in the local tangent plane. In the DTS model, the nematic can affect the membrane local deformation in the direction it is oriented ($\hat{n}$) as well as in the direction perpendicular to itself in the plane ($\hat{t}$) of the membrane. The effect of these nematic inclusions on the membrane curvature formation is modeled in terms of penalties to curvature formation in these two orthogonal directions. In short, the energy for membrane and protein system is given as below.

Preprints (www.preprints.org) | NOT PEER-REVIEWED | Posted: 22 August 2022 doi:10.20944/preprints202208.0366.v1

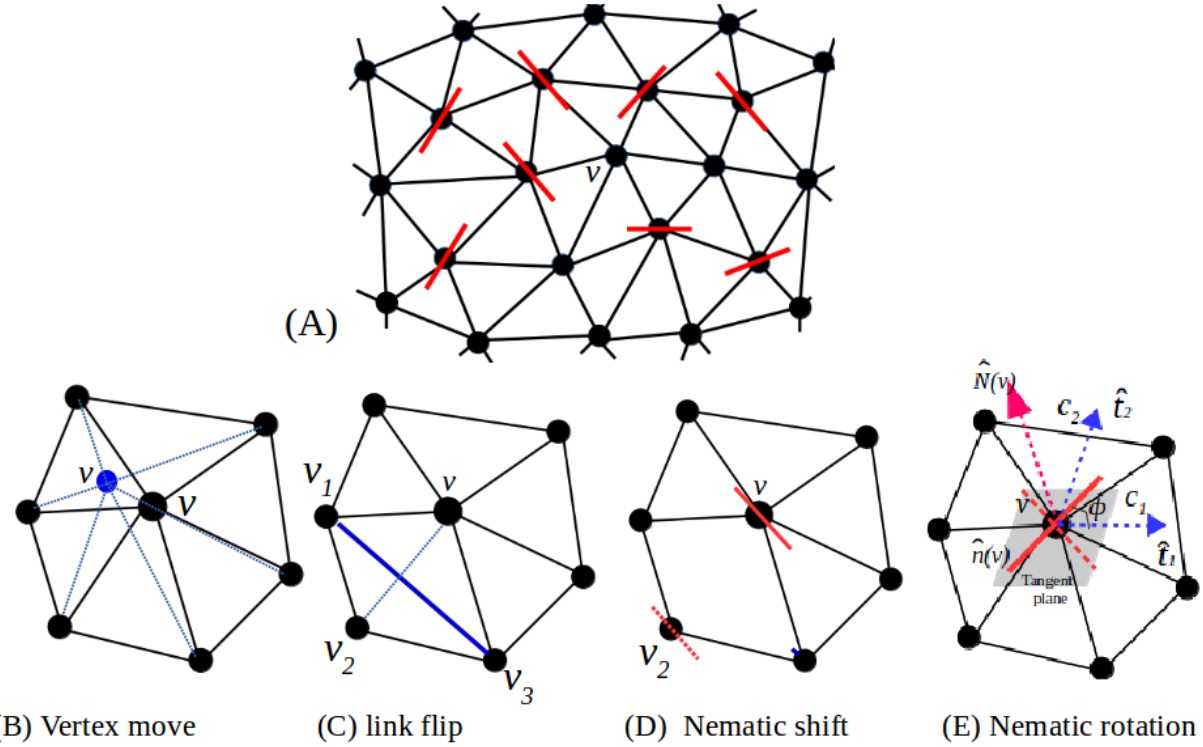

FIG. 1: (A) A small patch of the triangulated sheet with nematics. (B-E) The Monte Carlo moves for the energy minimization are vertex displacement, link flip, nematic shift, and nematic rotation

$$E_2 = \int \left(\frac{\kappa_\parallel}{2}(H_\parallel - c_\parallel)^2 + \frac{\kappa_\perp}{2}(H_\perp - c_\perp)^2 \right) dA, \tag{2}$$

where $\kappa_\parallel$ and $\kappa_\perp$ are the induced membrane bending rigidity and $c_\parallel$ and $c_\perp$ are the induced intrinsic curvatures along $\hat{n}$ and $\hat{t}$, respectively. $H_\parallel$ and $H_\perp$ are the membrane curvatures in the direction of $\hat{n}$ and $\hat{t}$, where $H_\parallel = c_1 \cos^2\phi + c_2 \sin^2\phi$ and $H_\perp = c_1 \sin^2\phi + c_2 \cos^2\phi$. As mentioned before, c_1 and c_2 are the local principal curvatures on the membrane surface along the orthogonal principal directions $\hat{t}_1$ and $\hat{t}_2$ as shown in Fig. 1. Here, ϕ is the angle between the direction of nematic orientation $\hat{n}$ and the principal direction $\hat{t}_1$.

The nematic-nematic interaction, which presents the interaction between protein molecules, is formulated based on the Frank's free energy for nematic liquid crystals[102].

Preprints (www.preprints.org) | NOT PEER-REVIEWED | Posted: 22 August 2022 doi:10.20944/preprints202208.0366.v1

$$E_3 = \int \sum_{k=1}^{N} \Big(\frac{K_1}{2} (\tilde{\nabla}.\hat{n})^2 + \frac{K_3}{2} (\tilde{\nabla}.\hat{t})^2 \Big) dA, \tag{3}$$

where $\tilde{\nabla}$ is the co-variant derivative on the curved surface and K_1 and K_3 are the splay and bending elastic constants for the in plane nematic interactions, respectively. For computational convenience, the above equation is recast into a discrete form[102] and expressed as the following.

$$E_3 = -\epsilon_{LL} \sum_{i>j} \Big(\frac{3}{2} (\hat{n}_i.\hat{n}_j)^2 - \frac{1}{2} \Big), \tag{4}$$

where ϵ_{LL} is strength of the nematic-nematic interaction with a constant approximation ($K_1 = K_3$). The sum $\sum_{i>j}$ is over all the nearest neighbour (i, j) vertices on the triangulated grid, promoting alignment among the neighbouring orientation vectors.

The total energy is the sum of these three energy (E_1, E_2, E_3). The Hamiltonian can also be augmented to explore features such as effect of surface tension and pressure difference $(P_{in} - P_{out})$ on membrane deformation and protein arrangement by including the additional term $\int \sigma.dA$ and $\int V.dP$ in the Hamiltonian formulation[97,100,103]. The area and volume conservation can also be applied by adding $\alpha_1 A^2 (1 - \frac{A_0}{A})^2$ and $\alpha_2 V^2 (1 - \frac{V_0}{V})^2$. Here A, V are are actual area and volume of the vesicle and A_0, V_0 are the cutoff value of area and volume.

B. Monte Carlo simulation details

Monte Carlo (MC) optimization technique is used to solve the Hamiltonian and arrive at the energy minimized membrane deformation. Four independent Monte Carlo moves for the energy minimization are required to evolve the shape of dynamically triangulated surfaces with nematics and reach the minimum energy configuration. These MC moves are (i) vertex move, (ii) bond flips, (iii) nematic shift and(iv) rotation. These MC moves provide the shape relaxation and fluidity in the system. Fig.1(A) shows a small patch of the triangulated sheet

 doi:10.20944/preprints202208.0366.v1

with nematics, where each vertex is connected with neighboring vertices with tethers.

1. In the first MC move, a randomly chosen vertex v is displaced inside a cubical box, which is centered at the vertex and shown in Fig1(B). The move takes the the membrane towards equilibrium.

2. In the second MC move, a set of two neighboring triangles are chosen and the common tether in between them is replaced by a new tether, which is created by a new connection in between two other non connected vertices. Fig. 1(C) shows the link flip. In this case, the tether between v and v_2 is replaced by creating new link between v_1 and v_3. This move guarantees that the vertex displacement is not controlled by the tether connection with its neighbors and thus ensures the fluidity in the system.

3. The third MC move allows the nematic shift from one vertex to another. This move is shown in Fig. 1(D) where the nematic from vertex v_2 is shifted to vertex v. This move also allows the membrane towards equilibrium and is important for diffusion of proteins on the membrane surface.

4. The fourth MC move allows the nematic rotation in the local tangent place of the vertex v. This move is shown in Fig. 1(E) where the nematic from vertex v is changing the orientation.

C. Curvature calculation

A discretized approach must be used to calculate the mean curvature in the DTS framework. There are several methods for calculating the mean curvature of a membrane surface, including calculating the overall curvature using triangle normals[86], discretization of mean curvature at any vertex[104], and principal curvature at any vertex of a triangulated surface[105]. For sake of completion, we provide the details of the method used in the original DTS model developed by Ramakrishnan and co-authors[105]. In this method, the mean curvature at a vertex v is calculated using a shape operator $S_v(v)$ with the mean of principal curvatures

Preprints (www.preprints.org) | NOT PEER-REVIEWED | Posted: 22 August 2022 doi:10.20944/preprints202208.0366.v1

$C_1(v)$ and $C_2(v)$ at that vertex.

$$S_v(v) = \frac{1}{A(v)} \sum_{\{e\}_e} W(e) P(v)^T S_e(e) P(v), \tag{5}$$

where area of the vertex A(v) = $\sum_{\{f_v\}} A(f)/3$ and the weight factor for an edge $W(e) = \hat{N}(v).\hat{N}(e)$. The projection operator (e) projects the $S_e(e)$ into tangent plane, where $p(v) = I - \hat{N}(v) \otimes \hat{N}(v)$. $S_e(e) = H(e)[\hat{R}(e) \times \hat{N}(e)][\hat{R}(e) \times \hat{N}(e)]$ is the discretized shape operator at an edge e with $H(e) = 2|R(e)| \cos(\Phi(e)/2$. $\hat{R}(e)$ is the unit vector along the edge e and $\hat{N}(v)$ is a unit normal vector calculated from the face normal $\hat{N}(f)$ and weight factor proportional to face area $A(f)$ at face f. $\hat{N}(e)$ is an unit normal vector to the edge e calculated by vector summation of the face normal adjacent to the edge e. $S(v)$ is converted from global coordinates to local coordinates using Householder transformation. The eigenvalues and eigenvectors of $S_v(v)$ are the principal curvatures $c_1(v)$ and $c_2(v)$ and directions $\hat{e}_1$ and $\hat{e}_2$, respectively.

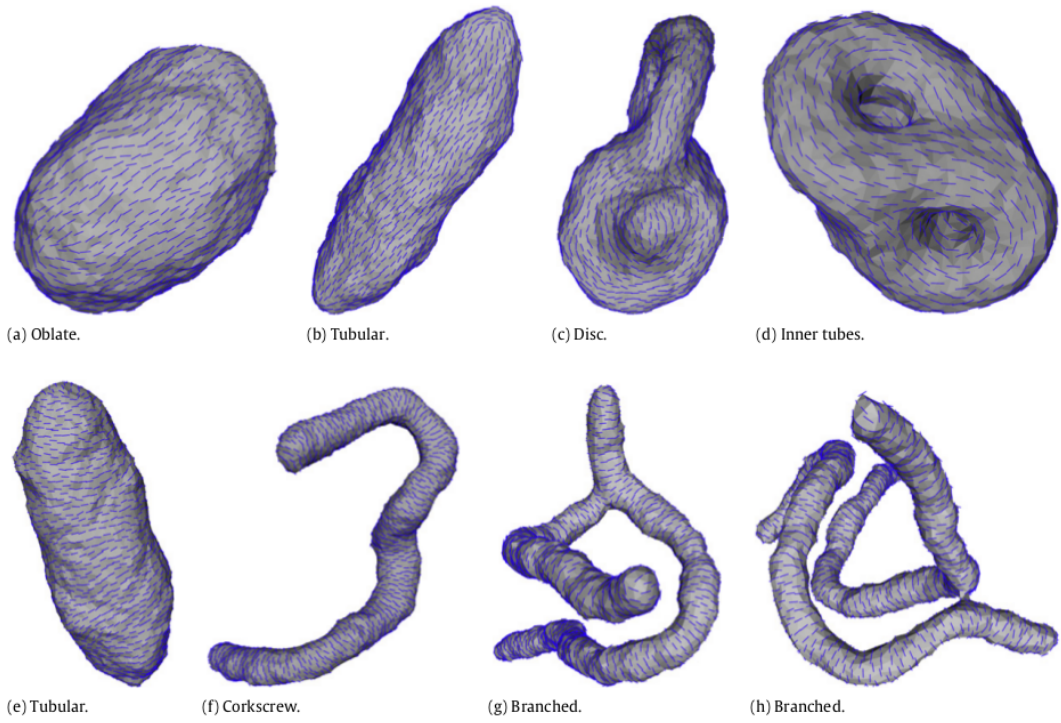

FIG. 2: Deformed vesicle morphologies obtained by Monte Carlo simulations with the different values of intrinsic curvatures (a) 0, (b) -0.3, (c) -0.4, (d) -0.6, (e) 0.2, (f)0.4, (g) 0.5 and(h) 0.6. Other parameters are $\kappa = 10$, $\kappa_{\parallel} = 10$ and $\epsilon_{LL} = 3$ in k_BT units. *Source*- Image is reprinted from[95] with permission of The Royal Society of Chemistry.

Preprints (www.preprints.org) | NOT PEER-REVIEWED | Posted: 22 August 2022 doi:10.20944/preprints202208.0366.v1

IV. VARIOUS USE CASES OF DTS MESOSCOPIC MODEL

A. Vesicle deformation due to linear aggregation of curvature proteins

DTS model is particularly suited to study mechanisms underlying the membrane remodelling due to scaffold proteins such as those belonging to BAR domain family. The DTS-based mesoscopic modeling provides mechanistic insights behind the related *in vitro* experiments. Fig.2 shows the equilibrium results of deformed vesicle due to curvature-forming scaffold proteins after MC optimization of the Hamiltonian functional. Here, the different shapes are obtained due to different values of intrinsic curvature $c_{\parallel}$ of the scaffold. In all the cases shown in Fig. 2, the bending rigidity of the membrane is kept at 10 k_BT with weak protein-protein interaction at 3 k_BT. The induced bending rigidity $\kappa_{\parallel}$ (or the protein membrane interaction in the lateral direction of the protein) is also kept at 10 k_BT. In the examples shown here, we assume that the protein does not cause curvature in the perpendicular lateral direction. As such, the other intrinsic curvature $c_{\perp}$ and induced bending rigidity $\kappa_{\perp}$ both are absent. In Fig. 2(a), the value of $c_{\parallel}$ is 0. This models a flat scaffold protein with no curvature. As such, in this case, the nematics are trying to impose their zero curvature on every vertex but due to closed configuration of the vesicle, it is not possible to get the 0 curvature value on every vertex. As a result, oblate shape is the minimum energy configuration shape with these parameters. The intrinsic curvatures value for Fig. 2(b-d) are $-0.3, -0.4, -0.6$, respectively. The lower panel shapes (Fig. 2(e-h)) are obtained due to positive value of $c_{\parallel} = 0.2, 0.4, 0.5, 0.6$, respectively. So it is clear from Fig. 2 that tubulation occurs with high value of $c_{\parallel}$. Vesicle deformation and tubulation is also possible with the less density of nematics[95]. Protrusion and invagination depend on the sign of the intrinsic curvature $c_{\parallel}$ of the scaffold protein. Invaginations occurs with the negative value of $c_{\parallel}$ and the outside tubulation occurs with the positive value of $c_{\parallel}$.

B. Vesicle deformation due to bundling of proteins.

In this use case, we discuss curvature proteins that can form bundles together by aligning laterally with each other and in some cases can also lead to curvatures formation in the membrane. FtsZ is one of the example of these proteins that forms a ring-like assembly at

Preprints (www.preprints.org) | NOT PEER-REVIEWED | Posted: 22 August 2022 doi:10.20944/preprints202208.0366.v1

the putative location of bacterial cell division. In reconstitution experiments, it has been found that membrane tubulation occurs when FtsZ protein filaments bind to the liposome[106]. Invagination and tubulation depend on whether the membrane anchors are attached to the C terminal or the N terminal of the protein filaments, which determines the effective curvature of the protein.

Fig.3 shows the equilibrium shapes of the deformed vesicle obtained by MC simulations under the area and volume conservation. Here, the initial configuration is the spherical triangulated vesicle with randomly oriented nematics on every vertex. The induced bending rigidities $\kappa_{\parallel}$ and $\kappa_{\perp}$ are 35 k_BT and 25 k_BT, respectively. For outward tubulation, the intrinsic curvatures $c_{\parallel}$ and $c_{\perp}$ are -0.05 and 1.0, respectively. The nematic-nematic interaction ϵ_{LL} is 3 k_BT. Fig. 3(a-c) and Fig. 3(a-e) show the outward and inward tubulation, respectively. Although intrinsic curvature $c_{\parallel}$ has non zero value, the tubulation here is controlled by the $c_{\perp}$. In these examples, a clearly visible arrangement of the nematics along the length of the tubes was observed both for tubulation and invaginations[97]. The total number of tubes are controlled by $c_{\parallel}$, $c_{\perp}$ and ϵ_{LL} parameters[97]. The spacing between the tubes is controlled by the $c_{\parallel}$ and the radius of the tubes can be changed by $c_{\perp}$. Spacing between the tubes is also controlled by the ϵ_{LL} because ϵ_{LL}, which determines the protein-protein interactions, allows the nematics to arrange parallel to each other. At high ϵ_{LL} values, the nematics cover more space between the tubes that allows them to assemble in the energetically favorable parallel arrangements leading to reduced number of tubes formation.

A key aspect of the nematic membrane model is its ability to induce curvature even when the directional spontaneous curvatures are both set to zero (i.e. $\kappa_{\parallel} = \kappa_{\perp} = 0$)[107]. In this case the deformation is induced by the parallel arrangement of the ordered in-plane nematic fields. Fig. 4 shows the vesicle deformation with out directional spontaneous curvatures. Here the other parameters are $\kappa = 10$ and $\epsilon_{ll} = 10$ in k_BT units. According to the hairy-ball theorem[108], filaments cannot be tangentially arranged on a closed surface without forming topological defects and the sum of the topological charge of these defects is equal to 2. In Fig. 4, the deformation of the spherical vesicle is driven by the nematic-nematic interaction term. Here, all the nematics are trying to arrange parallel to each other and four +1/2 defects are already formed due to the closed configuration. So in the deformed morphology, all four defects are arranged at the corner due to parallel arrangement of nematics and a

Preprints (www.preprints.org) | NOT PEER-REVIEWED | Posted: 22 August 2022 doi:10.20944/preprints202208.0366.v1

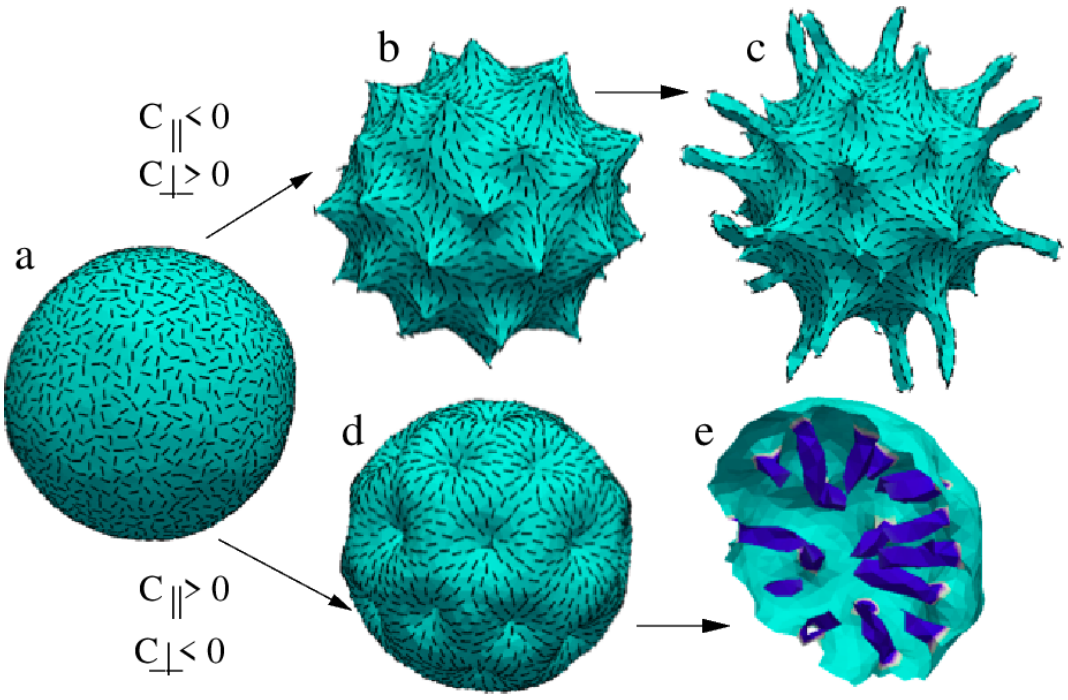

FIG. 3: Deformed vesicle shapes obtained by Monte-Carlo simulation under the area and volume conservation. a-c and a-e show the outward and inward tubulation respectively. Intrinsic curvatures $c_{\parallel}$ and $c_{\perp}$ for a-c and a-e are (-0.05,1.0) and (0.05,-1.0) respectively. Other parameters are $\kappa_{\parallel} = 35$, $\kappa_{\perp} = 25$ and $\epsilon_{LL} = 3$ in k_BT units. In these tubulated and invaginated structures, the protein arrangement is in the longitudinal direction of the membrane tube. *Source*- Image is reprinted from[97] with permission of American Physical Society.

tetrahedral morphology is obtained as the result of deformation.

C. Vesicle deformation due to chiral proteins.

Several curvature sensing and curvature-inducing protein in the vesicular transport pathways are chiral in nature including the proteins from BAR/Nexin family with the membrane adaptor proteins on them. Chirality induced tubulation and budding have been conjectured from observation made in experimental systems[109–112] and also explored in theoretical studies and mesoscopic modeling[99,113,114]. In a recent work from Anirban Sain and co-workers[99], organization of chiral proteins both on the rigid surface and deformable surfaces is studied and mechanisms leading to membrane deformation due to short surface binding chiral protein filaments was explored. The DTS Hamiltonian is extended to allow for explicit modeling of chiral nematics on membrane surface using the additional terms in Eqn. (6) as shown below.

Preprints (www.preprints.org) | NOT PEER-REVIEWED | Posted: 22 August 2022 doi:10.20944/preprints202208.0366.v1

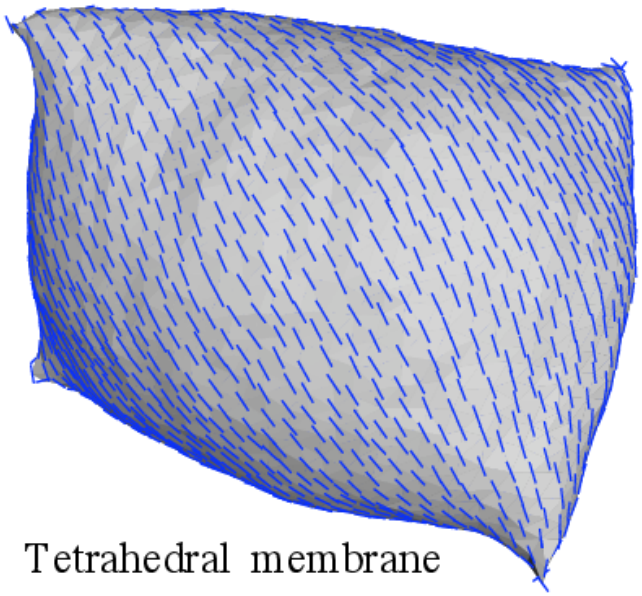

FIG. 4: Deformed vesicle without the directional spontaneous curvatures ie $\kappa_{\parallel} = \kappa_{\perp} = 0$. Here four $+1/2$ defects remodel the surface into a tetrahedron. other parameters are $\kappa = 10$ and $\epsilon_{ll} = 10$ in k_BT units. *Source*- Image is reprinted from[107] with permission of Wiley Online Library.

$$E_{Chiral} = \int \frac{\kappa}{2}(2H)^2 dA + \sigma A + \Delta P.V - \epsilon_{LL} \sum_{nn} (\hat{n}_i.\hat{n}_j)^2 \\ -2\epsilon_C q_0 \sum_{nn} \hat{r}_{ij}.(\hat{n}_i \times \hat{n}_j)(\hat{n}_i.\hat{n}_j) \quad (6)$$

where the first term is the membrane bending energy which is already discussed in the model section. Second and third terms are the surface tension energy and pressure difference $\Delta P = P_{out} - P_{in}$ energy terms. The fourth term is discrete form of the combination of splay and bending energy for nematics. ϵ_{LL} is the strength of nematic-nematic interaction. Last term is the discrete form of the twist energy of nematics, originally proposed by the van der Meer[115].ϵ_C is the strength of chiral term and q_0 is the intrinsic chirality. $\hat{n}_i$ and $\hat{n}_j$ are the two neighbor nematics and free to rotate in the local tangent plane. r_{ij} is the distance between vertices where the $\hat{n}_i$ and $\hat{n}_j$ are fixed. It is worth noting that special considerations in formulation are required because chirality is a three dimensional feature and cannot be simply captured by the movement of nematics in the local tangent(2D) plane

Preprints (www.preprints.org) | NOT PEER-REVIEWED | Posted: 22 August 2022 doi:10.20944/preprints202208.0366.v1

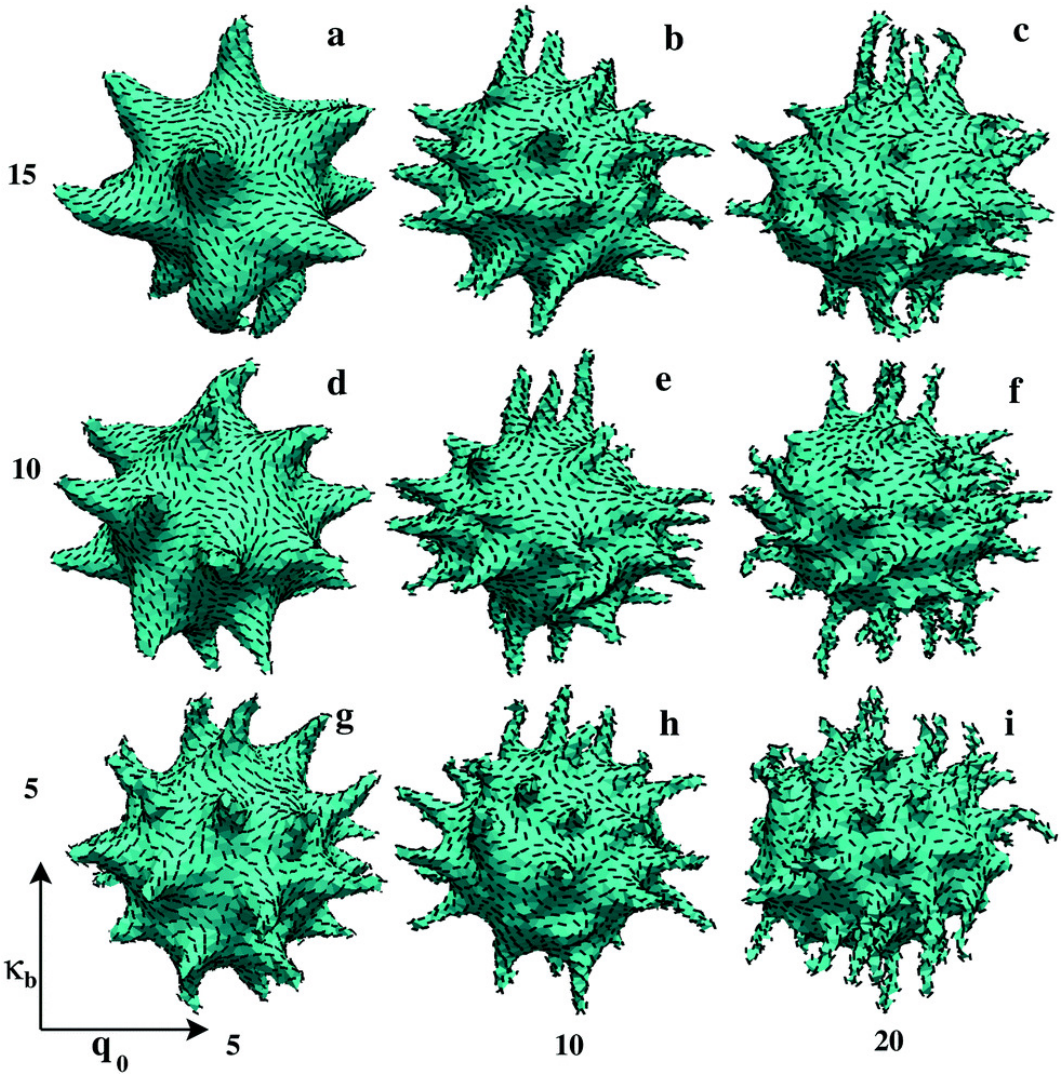

FIG. 5: Vesicle deformation due to chiral nematics under the constraint of volume conservation. All the shapes are the function of intrinsic chirality q_0 and membrane bending rigidity κ. Conical protrusions are formed with high value of κ and low value of q_0. tubulation is possible with the high value of q_0. *Source*- Image is reprinted from[99] with permission of The Royal Society of Chemistry.

of a flat surface. With the new formulation, even if the nematics rotate in the local tangent plane of a curved surface, it is now possible to capture the chiral behavior of nematics.

Fig. 5 shows the equilibrium shapes of the deformed vesicle, obtained by Monte-Carlo simulations. Here the energy function is scaled by ϵ_C ($\epsilon_C = 1$) for the simulation. The other parameters ϵ_{LL} and σ are 1 and 0.5, respectively. These results are obtained under the constraint of volume conservation. It is clear from Fig. 5 that different size of

Preprints (www.preprints.org) | NOT PEER-REVIEWED | Posted: 22 August 2022 doi:10.20944/preprints202208.0366.v1

conical protrusions are formed with low values of q_0 and for a range of κ/ϵ_C. Tubulation is only possible with the high value of q_0 and the nematics form the helical arrangement on the tubes. In their recent paper, Sain and co-workers also show the deformed vesicle can results without volume constraint with the same parameter of Fig. 5 where they have found fully tubulated structure with low value of κ/ϵ_C[99]. They have also captured the effect of pressure difference in the Hamiltonian. If the pressure difference ΔP is negative, then conical protrusions are formed. These conical protrusions convert into tubes with the increase of ΔP. So it is clear that tubulation is also possible with out curvature of proteins and it depends on the bending rigidity κ, intrinsic chirality q_0 and the pressure difference ΔP.

D. Vesicle deformation due to mixture of different proteins.

Membrane remodeling requires highly orchestrated biochemical interactions between multiple proteins and lipids molecules. As discussed earlier, Clathrin-mediated endocytosis (CME) is a paradigmatic example where a total of more than fifty proteins are either individually or in complex are "called upon" from the cytosolic reservoir in a highly coordinated manner at different stages of the endocytosis process[2,8,116]. Another example, also mentioned above, is the three way junction of the tubes in endoplasmic reticulum. These junctions are stabilized by lunapark (Lnp1p) protein while the tubes are stabilized by the reticulon and reep proteins[117,118]. These proteins have different parameter like curvature and membrane binding affinities. Similarly, Sorting Nexin (SNX) and BAR domain families of proteins are ubiquitous in the endocytic recycling pathways and play important roles for the vesicular and cargo transport processes[116,119–124]. BAR families of proteins have a wide range of curvature values such as F-BAR and N-BAR[3,116] with positive curvature and I-BAR[125,126] having negative curvatures, to name a few. These proteins induce and stabilise different degrees of local and non-local curvatures to create the complex vesicular morphology needed in the cellular context[127–131]. For example, Feng-Ching Tsai and coworkers recently showed how multiple proteins such as IRSp53, VASP, Actin and Fascin work in a tightly regulated manner for formation and maintenance of filopodia protrusions[126]. Generally, due to the non-trivial nature of probing these processes in experiments, exact interplay between different scaffold proteins

Preprints (www.preprints.org) | NOT PEER-REVIEWED | Posted: 22 August 2022 doi:10.20944/preprints202208.0366.v1

in creating and maintaining membrane deformation is not studied extensively except for a few recent limited reconstitution experiments (to the best of our knowledge)[9,10,12,13,132]. Also, only limited theoretical and computational work is visible where more than two kinds of scaffold proteins are shown to interplay on membrane surface and induce curvatures[74,78,133,134]. Besides, due to the presence of long unstructured linkers regions between well-folded domains of scaffold proteins, the effective curvature can be thought to have a distribution rather than a fixed value[135,136]. Scaffold proteins such as Amphiphysin1 from the BAR family[119], Epsin N-terminal homology domain[137], dynamic and EHD proteins[47,111,138,139] and AP180[137] - all have multiple disordered region and contains sizeable intrinsically disordered regions that causes the effective curvature to fluctuate in the thermal environment. As such, it would be useful to have a mesoscopic model that accounts for curvature fluctuations as well as presence of multiple types of scaffold proteins in the reservoir to allow for study of interplay between the proteins leading to curvature formation.

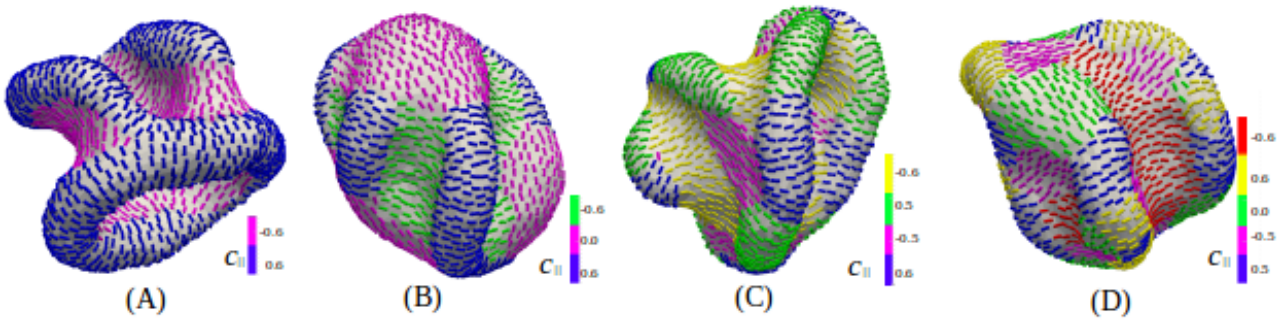

FIG. 6: Panel shows the deformed vesicle morphologies obtained by Monte Carlo simulation due to two, three, four and five different curvatures of proteins with curvature values (± 0.6), $(0, \pm 0.6)$, $(\pm 0.5, \pm 0.6)$ and $(0, \pm 0.5, \pm 0.6)$. Different colors show the different values of protein's curvature. Other parameters are $\kappa = 20$, $\kappa_{\parallel} = 10$ and $\epsilon_{LL} = 3.5$ in $k_B T$ unit.

Recently, our group has extended the nematics based mesoscopic modelling that can be used to study membrane remodelling due to mixture of differently curved proteins[103]. In this section, we briefly present the method and its application. Here different value of proteins numbers, proteins curvatures, membrane protein interactions and protein-protein interactions can be chosen. This extension helps to understand how different kinds of curvature generating proteins with different interactions work in the coordinated manner to generate the desired membrane morphology. If total number of different curvature proteins is ρ then

Preprints (www.preprints.org) | NOT PEER-REVIEWED | Posted: 22 August 2022 doi:10.20944/preprints202208.0366.v1

ρ=$\Big[\rho_1 + \rho_2 + ... \ ... + \rho_N\Big]$ where $\sum_{i=1}^{n} \rho_i \leq n_v$ and $\rho_1, \rho_2, ...\rho_N$ are the number of different curvature proteins(nematics) and n_v is the total number of the vertices on the triangulated surface. Here we have one nematic on every vertex. So the total number of nematics cannot exceed the total number of vertices. Different proteins can have different curvatures, induced membrane bending rigidities and interactions.

Denoting $\kappa_{\parallel 1}, \kappa_{\parallel 2}.....\kappa_{\parallel N}$ and $c_{\parallel 1}, c_{\parallel 2}.....c_{\parallel N}$ as the induced bending rigidities and curvatures of proteins along the direction of the nematics, respectively and $\kappa_{\perp 1}, \kappa_{\perp 2}.....\kappa_{\perp N}$ and $c_{\perp 1}, c_{\perp 2}.....c_{\perp N}$ as induced bending rigidities and curvatures, respectively in the perpendicular direction of nematics, we express the rigidity and curvature as a vector space given as: $\kappa_{\parallel}$=$\Big[\kappa_{\parallel 1} \ \kappa_{\parallel 2} \ ... \ ... \ \kappa_{\parallel N}\Big]$, $\kappa_{\perp}$=$\Big[\kappa_{\perp 1} \ \kappa_{\perp 2} \ ... \ ... \ \kappa_{\perp N}\Big]$, $c_{\parallel}$=$\Big[c_{\parallel 1} \ c_{\parallel 2} \ ... \ ... \ c_{\parallel N}\Big]$, $c_{\perp}$=$\Big[c_{\perp 1} \ c_{\perp 2} \ ... \ ... \ c_{\perp N}\Big]$. The cross-interaction term among the various proteins is written as a matrix:

$$\epsilon_{LL} = \begin{bmatrix} \epsilon_{LL}^{1,1} & \epsilon_{LL}^{1,2} & ... & ... & \epsilon_{LL}^{1,N} \\ \epsilon_{LL}^{2,1} & \epsilon_{LL}^{2,2} & ... & ... & \epsilon_{LL}^{2,N} \\ ... & ... & ... & ... & ... \\ ... & ... & ... & ... & ... \\ \epsilon_{LL}^{N,1} & \epsilon_{LL}^{N,1} & ... & ... & \epsilon_{LL}^{N,N} \end{bmatrix}$$

where $\epsilon_{LL}^{i,i}$ is the interaction between same curvature of nematics (same interaction) and $\epsilon_{LL}^{i,j}$ is the interaction between different curvature of nematics (cross interaction). Here we have considered both cases $\epsilon_{LL}^{i,i} > \epsilon_{LL}^{i,j}$ and $\epsilon_{LL}^{i,i} < \epsilon_{LL}^{i,j}$ and show that how they affect the membrane deformation. Fig. 6 shows vesicle shapes due to different numbers of proteins.

E. Vesicle deformation due to cytoskeletal filaments

Nematics as protein inclusions on the surface of the membrane has been the most common form of protein-induced membrane curvature formation studies carried out using DTS method. Recently, the DTS framework has been extended to explore how semi-rigid filaments could modulate vesicle morphology[98]. The work is presented for sickling hemoglobin fibres (HbS) but is extendable to other filaments such as a microtubules and filamentous actin as well. In this work, the DTS method is used to model the effect of long semi-rigid hemoglobin

Preprints (www.preprints.org) | NOT PEER-REVIEWED | Posted: 22 August 2022 doi:10.20944/preprints202208.0366.v1

protein filaments inside the the red blood cell (RBC) to unravel the factors leading to pathologically debilitating deformation of RBCs. While the usual closed dynamically-triangulated network model is used for vesicular biological membrane, a worm-like chain model is used for the hemoglobin filament. This is a transformative addition to the DTS framework as it could allow the modeling of membrane deformations due to filamentous cytoskeletal proteins. Using this new construction, Sain and co-workers have explored the equilibrium configuration of the filament- vesicle hybrid system. Besides the oft-studied effects of membrane modulus and filament rigidity on the equilibrium shape of RBC, the effect of 3D confinement of the helical filament conformations and the surface area versus volume of membrane are well explored in this work. These features seem to have important relevance to sickle cell anemia (SCA).

Different shapes of red blood cells are associated with many disease like myelofibrosis, anemia and thalassemia. Here we discuss SCA, which is a serious blood disease and occurs when the discocytes shaped RBC are converted into sickle shapes. It happens due to the abnormal growth of the semi-rigid hemoglobin (HbS) fibers inside the RBC. When oxygen deficiency occurs inside the RBC then the molecules of hemoglobin-S (HbS) nucleate and polymerize abnormally[140] and form a long chain of HbS fibers. This HbS fiber semi rigid chain push the RBC membrane from inside and try to deform it. The Hamiltonian free-energy of the combined system is written as:

$$\tilde{E} = \frac{1}{4}\oint_S (\tilde{C}_1 + \tilde{C}_2)^2 d\tilde{A} + \frac{\bar{\kappa}\pi}{\kappa_b}(\Delta a - \Delta a_0)^2 + \kappa_B T \frac{l_p}{2\Delta} \sum_{i=1}^{M-1} (\vec{t}_{i+1} - \vec{t}_i)^2 \tag{7}$$

In the equation above, energy is scaled by $8\pi\kappa_b$. First term is the bending energy of vesicle taken from the classical Helfrich-Canham energy . The second term is defined based on the non-local bending energy which is caused by the area difference between the lipid bilayers. Here $\Delta a = \frac{\Delta A}{\Delta A_s}$, $\Delta a_0 = \frac{\Delta A_0}{\Delta A_s}$ where $\Delta A_s = 8\pi h \rho_s^3$ is the area difference of a sphere and $\Delta A = h \oint (C_1 + C_2) dA$ is the area difference between the two phospolipid monolayers, whose neutral planes are separated by a length h. The third term is represented by worm-like-chain

Preprints (www.preprints.org) | NOT PEER-REVIEWED | Posted: 22 August 2022 doi:10.20944/preprints202208.0366.v1

model, which represents the bending energy of the filament, where $\vec{t_i}$ are link vectors and Δ is the link length such that the filament length is $L = M\Delta$ (M is the linearly connected links).

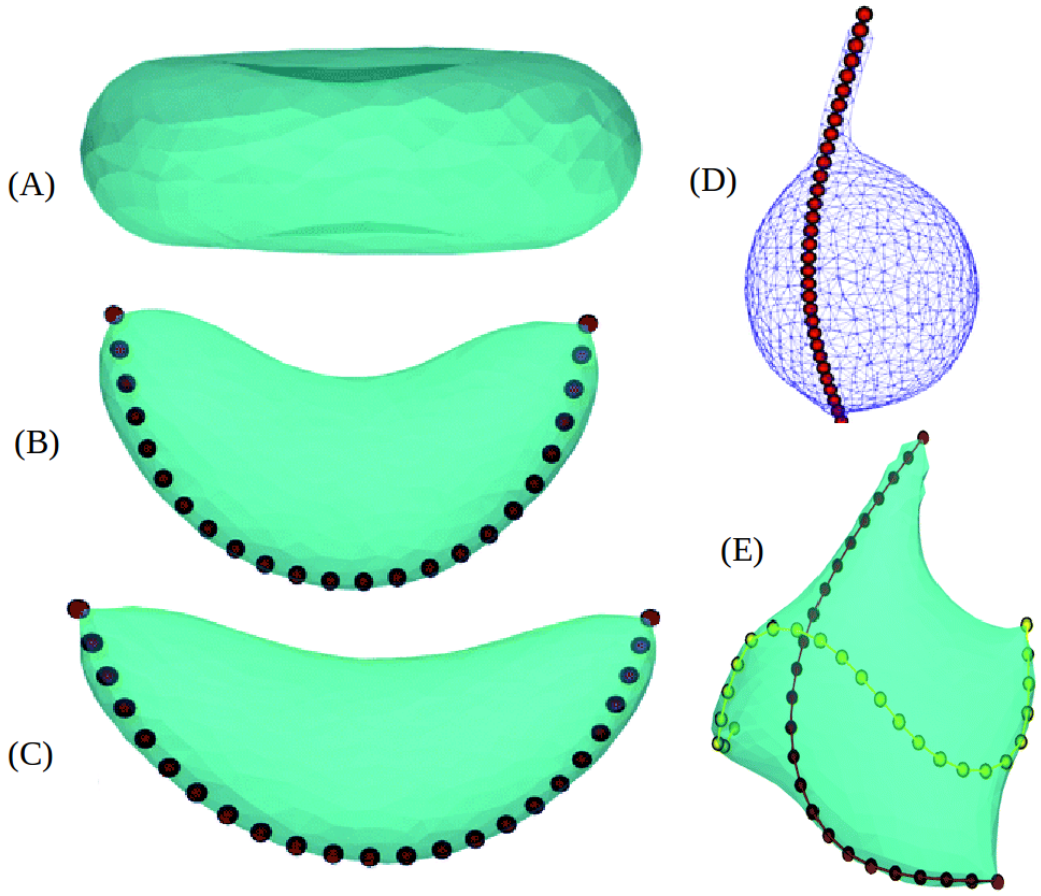

FIG. 7: (A) Normal biconcave RBC (discocyte) shape generated with the fix value of area and volume ratio. (B) and (C) show deformed RBC with a confined WLC chain inside where only l_p is changing from $2.9l_p^0$ to $5.8l_p^0$. (D) Vesicle deformation due to long filament here the area and volume ratio is higher then B and C .(E) Multipolar RBC shape due to two confined filaments. *Source*- Images are adapted from[98] with permission of The Royal Society of Chemistry.

Sain and co-workers[98] show the shape deformation of RBC due to one and two HbS fiber chains and their data reveals that a single chain may not be enough to generate a sharp edge sickle like shape. Fig. 7A shows the normal biconcave RBC shape that is generated by fixed area and volume ratio. Fig. 7(B,C) show the deformed shape of RBC due to worm like chain with two different values of persistence length of the chain. Fig. 7D shows the membrane tubulation due to long filament. Here, the area-volume ratio is higher than Fig. 7B and C.

Preprints (www.preprints.org) | NOT PEER-REVIEWED | Posted: 22 August 2022 doi:10.20944/preprints202208.0366.v1

Fig.7E shows the shape deformation of RBC with two non interacting worm like chain.

F. Vesicle deformation due to peripheral filamentous proteins as in autophagy

Autophagy is a biological process used by the cell for recycling the cellular material[141–143]. It is initiated under stress condition such as nutrient starvation. Autophagy is also common in multiple disease like cancer, cellular aging, immune system and infection[144–147]. In this process, membrane deforms into a cup shaped double membrane shape to generate autophagosomes from phagophores. Experimentally, it has been found that fusion of few vesicle is a critical step to generate this shape. A "S" shaped curvature protein called "Atg9" mediates the formation of autophagosome. At the early stage of the process (before formation of fusion complexes), Atg1 sub complexes Atg17-Atg31-Atg29 remodels the membrane to generate cup shaped autophagosome. In a new framework that combines DTS membrane model with coarse-grained protein model, Bahrami and co-workers[148] model the formation of autophagosome due to "S" shaped polymer. The Hamiltonian energy of the combined system is given below.

$$E = 2\kappa \sum_{n_v}^{\alpha} \frac{(M_\alpha)^2}{A_\alpha} + K_A(1 - A/A_{ref})^2 + K_V(a - V/V_{ref})^2 - UA_{bd} + \frac{1}{2}K_{bond}\sum(\Delta L)^2 + \frac{1}{2}K_{ang}\sum(\Delta\theta)^2 + \frac{1}{2}K_{dih}\sum(\Delta\gamma)^2 \quad (8)$$

The first term represents the discrete form of Helfrich energy in a tessellated vesicle with n_v vertices. κ is bending rigidity, M_α is the curvature contribution of vertex α that is equal to $\frac{1}{4}\sum ijl_{ij}\phi_{ij}$ (where I_{ij} is the edge length, and ϕ_{ij} is the angle between two normal vectors of neighbor triangles sharing edge ij] and A_α. The second and third terms are stiff harmonic potentials used to preserve the area A and volume V of the vesicle at reference value A_{ref} and V_{ref}, respectively. K_A and K_V are stiffness coefficients of area and volume. The fourth term is binding energy, where U is the binding energy per unit area and A_{bd} is the total area

Preprints (www.preprints.org) | NOT PEER-REVIEWED | Posted: 22 August 2022 doi:10.20944/preprints202208.0366.v1

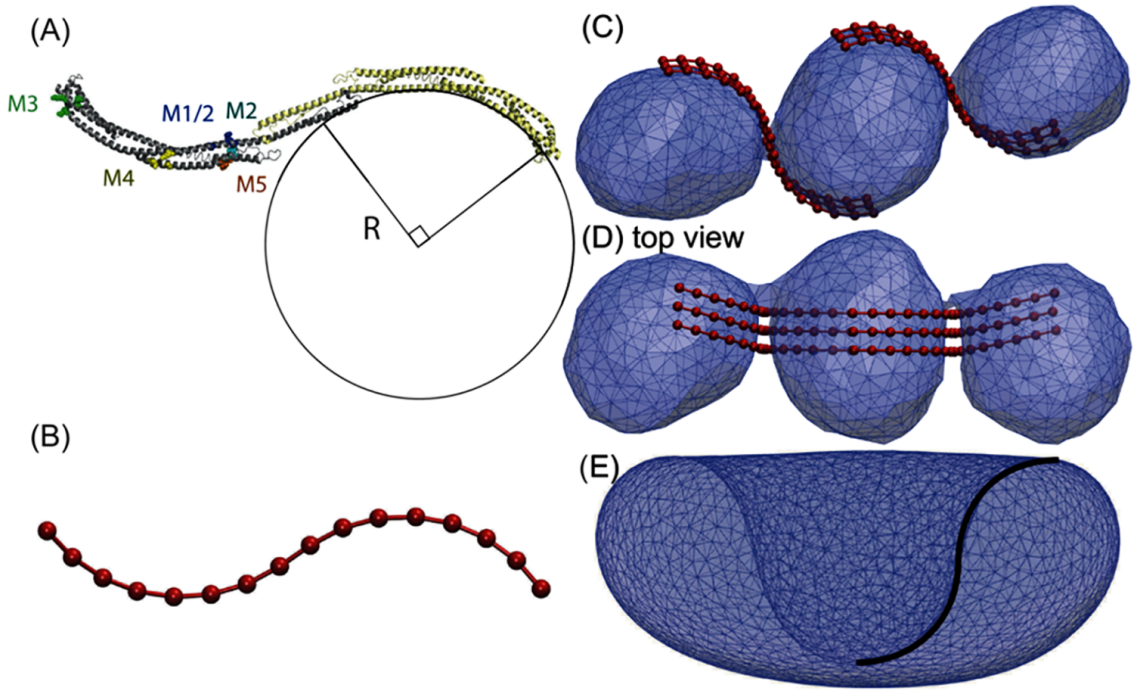

FIG. 8: (A) Atg17 dimer's "S" shape structure in ribbon representaion. (B)Coarse grained structure of Atg17 dimer. (C) and (D) Side and top view of just fused three vesicle tethered by two group of Atg17 three dimers. (E) Deformed vesicle in to cup shape due to Atg17 dimers. *Source*- Images are adapted from[148] with permission of Public Library of Science San Francisco, CA USA.

of the membrane adhered to the dimer beads. The fifth, sixth, and seventh terms are the internal potential energies that account for the fluctuations in bond length, bond angle, and dihedral angle, respectively.

Bahrami et al.[148] show that a minimum of three vesicles are required for fusion to generate phagophore shape and the role of S shaped Atg17 is critical to generate autophagosome. They have also shown autophagosome is not possible if Atg is absent or weakly binds to the membrane. This s shape of Atg17 is also important as they clearly show that autophagosome is not possible with the linear shape of Atg17. Fig. 8(A,B) show the ribbon representation and coarse grained representation of Atg17. Fig. 8C and D show the side and top views of three diffuse vesicles with the the "S" shaped Atg17 dimers. Fig. 8E shows the equilibrium bowl shape of vesicle due to atg17 dimers.

Preprints (www.preprints.org) | NOT PEER-REVIEWED | Posted: 22 August 2022 doi:10.20944/preprints202208.0366.v1

G. Deformation of flat membrane due to proteins and membrane-active agents

In all the previous examples of membrane remodeling, we have discussed the vesicle deformation due to surface bound proteins where the proteins are modeled as nematic field or long filaments. The effect of the proteins can also be introduced by the curvature field[149–152]. In this case, the elastic energy of the membrane-proteins includes a spontaneous curvature field H_0 that represents the curvature-inducing interactions between the protein and membrane. The elastic energy of Eq. 1 is modified as:

$$E = \int \Big(\frac{\kappa}{2}(H - H_0)^2 + \kappa_G G + \sigma\Big) dA, \tag{9}$$

H_0 can be defined as a shape function based on the modeling constraints. When the form of the spontaneous curvature field is a cosine function or a square-well function or an isotropic Gaussian function, then vesicular buds are formed under certain configurations. When an anisotropic (ellipse shaped) Gaussian dimple, or an anisotropic saddle shaped function is used as spontaneous curvature field then tubules are induced from membrane. The spontaneous curvature induced in the vicinity of the membrane at $\vec{r_m}$ due to a protein at $\vec{r_p}$ is represented as $H_0(\vec{r_m}, \vec{r_p}) = C_0 F(\vec{r_m}, \vec{r_p})$ with $F(\vec{r_m}, \vec{r_p}) = \exp(-r^2/\epsilon^2)$, $r = |\vec{r_m} - \vec{r_p}|$ and the $\epsilon^2/2$ is the variance of the Gaussian. Here, C_0 is the induced membrane curvature at $\vec{r_m} = \vec{r_p}$. In general, the function F can take any arbitrary form as imposed by the protein curvature field. Fig. 9(a-c) shows the equilibrium shapes of deformed planar membrane with the six protein fields. Here, the deformation occurs due to spontaneous curvature which is induced by the proteins for different magnitudes of the imposed curvature C_0 with fixed $\epsilon^2 = 6.3a_0^2$. The magnitudes of imposed curvature in Fig. 9(a-c) are $C_0 = 0.0, 0.4$, and $0.8a_0^{-1}$ respectively. Fig. 9(d-f) shows the equilibrium shapes of deformed planar membrane due to a fixed value of the magnitude of spontaneous curvature $C_0 = 0.8a_0^{-1}$. Different morphology are obtained due to different number of protein fields – $n = 2, 8$ and 14, respectively in Fig. 9(d-f). In Fig. 9(f), tubule is formed as the result of clustering of proteins. Here, a_0 is the length unit.

Preprints (www.preprints.org) | NOT PEER-REVIEWED | Posted: 22 August 2022 doi:10.20944/preprints202208.0366.v1

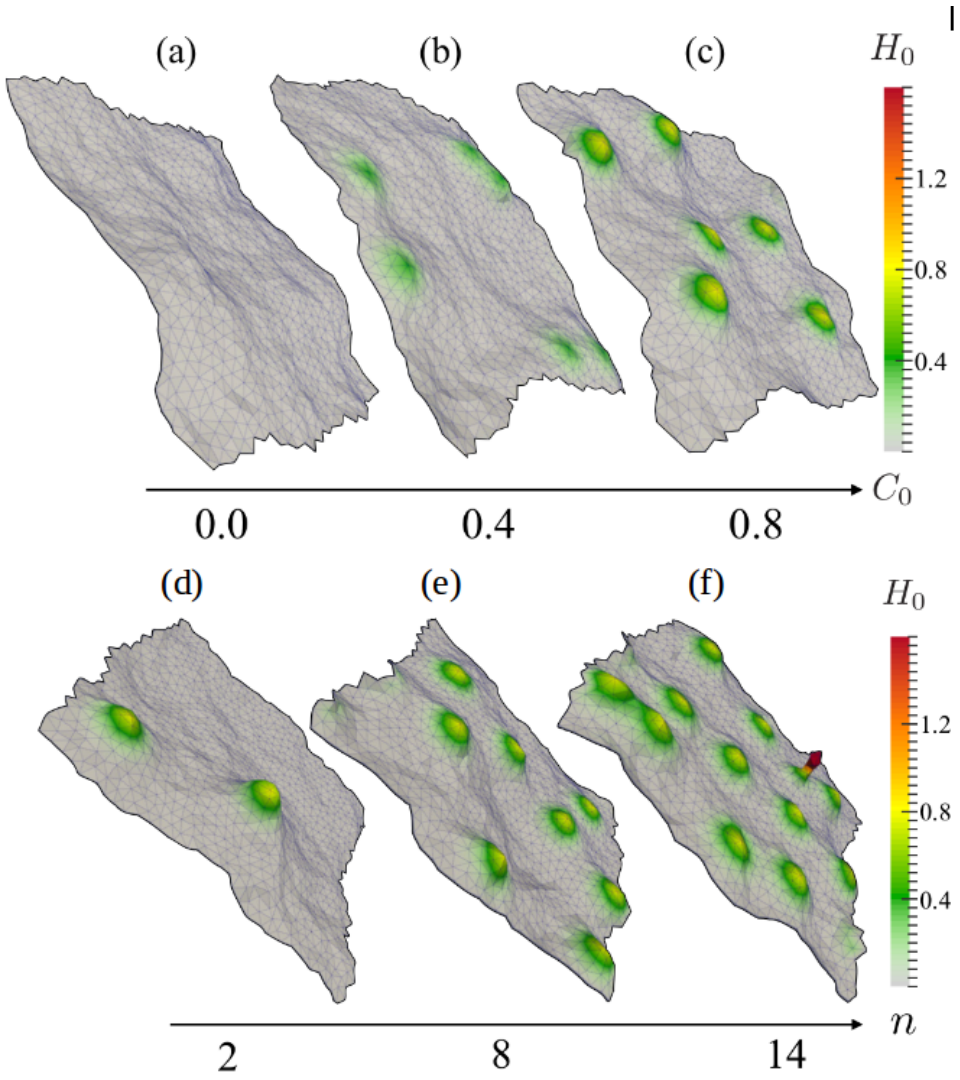

FIG. 9: Equilibrium shapes of the Deformed planar membrane obtained by Monte-Carlo simulation. In (a-c), the magnitudes of imposed curvature $C_0 = 0.0, 0.4$, and $0.8a_0^{-1}$ with the fixed number of protein fields $n = 6$. In (d-f), the magnitudes of imposed curvature is fixed $C_0 = 0.8a_0^{-1}$ while the protein fields are varying$n = 2, 8$ and 14. *Source*- Image is reprinted from[149] with permission of American Physical Society.

H. Deformation of multiple component membrane vesicle

Biological membrane is a multiple component system and contains multiple kind of lipids and molecules[154–160]. These components can also generate curvature in membrane[161]. In general, in all the examples discussed so far, we have assumed models that have single component membrane. There are a few examples in mesoscopic modeling literature where multi-component membrane is considered. A model was proposed by Iglic and co-workers

Preprints (www.preprints.org) | NOT PEER-REVIEWED | Posted: 22 August 2022 doi:10.20944/preprints202208.0366.v1

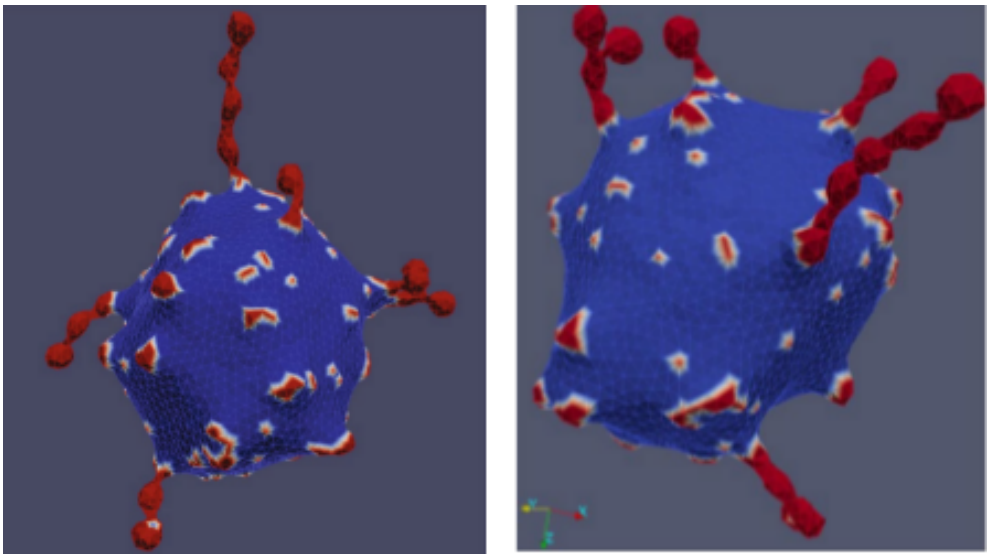

FIG. 10: Spontaneous vesicle deformation due to two component membrane system. One component has higher intrinsic curvature and the other one has the zero intrinsic curvature. Both are shown by red and blue color respectively.*Source*- Images are adapted from[153] with permission of Springer.

for multiple component system[162–164] with two different components system A and B. If the intrinsic curvatures of both component A and B are C^i_{1m} and C^i_{2m}, then the energy of membrane is given as:

$$E = \int \frac{\kappa(\phi)}{2}\Big[(H - H_m(\phi))^2 + (D - D_m(\phi))^2\Big]dS, \tag{10}$$

where $H = (C_1 + C_2)/2$ is the membrane mean curvature and $D = |C_1 - C_2|/2$ is the membrane curvature deviator. C_1 and C_2 are the membrane principal curvatures. $\kappa(\phi)$ is the membrane bending rigidity for the mixed component system. Here dS is the elementary area of the membrane and ϕ is the areal density of the component A. $H_m(\phi)$ and $D_m(\phi)$ are the intrinsic mean curvature and curvature deviator of membrane. $\kappa(\phi)$, $H_m(\phi)$ and $D_m(\phi)$ depend linearly on the ϕ. Here, $\kappa(\phi) = (\kappa^A - \kappa^B)\phi + \kappa^B$, $H_m(\phi) = (H^A_m(\phi) - H^B_m(\phi))\phi + H^B_m(\phi)$, and $D_m(\phi) = (D^A_m(\phi) - D^B_m(\phi))\phi + D^B_m(\phi)$ with κ^A and κ^B are the bending rigidities of the component A and B, respectively. $H^i_m = (C^i_{1m} + C^i_{2m})/2$ is the intrinsic mean curvature of the component i and $D^i_m = |(C^i_{1m} - C^i_{2m})|/2$ is the intrinsic curvature deviator of the component i, where i=A,B. Membrane free energy is associated with the entropy of mixing

Preprints (www.preprints.org) | NOT PEER-REVIEWED | Posted: 22 August 2022 doi:10.20944/preprints202208.0366.v1

and expressed as:

$$F_{mix} = \frac{k_B T}{a_0} \int \Big[\phi \; ln\phi + (1-\phi) \; ln(1-\phi)\Big] dS, \tag{11}$$

where k_B is the Boltzmann constant, T is the absolute temperature and a_0 is the area of a single nanodomain. The free energy functional is the sum of both energies. Mesarec and co-workers[153] show that vesicle deformation results when the membrane is composed of two isotropic constituents and one of the components has high intrinsic curvature (Red) and another has zero intrinsic curvature (Blue) in Fig. 10. The component which has higher curvature formed tubes while the zero curvature component arranged in between the tubes.

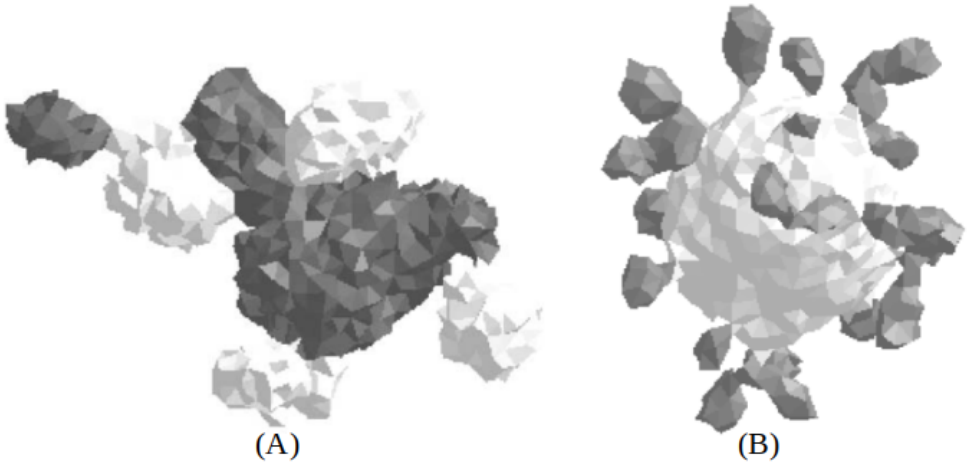

FIG. 11: Deformed morphologies of vesicle due to two component membrane system. Both component are shown by white and gray colors. (A) Both types of patches(component) have zero "spontaneous" curvature. (B) White patach has zero curvature while gray patches have nonzero "spontaneous" curvature. *Source*- Image is reprinted from[161] with permission of American Physical Society.

Multicomponent membranes are also studied by Lipowsky and co-workers in the triangulated membrane system[161]. In this work, the focus is on membranes that form intramembrane domains and undergo domain induced budding due to multiple components present in the membranes. Here, the membrane is modelled as triangulated surface and the two different components of membrane are denoted by the two different triangles a and b. Three types of Monte Carlo moves are used for the surface evolution (i)vertex move, (ii)link flip and (iii) exchange of triangles. First two MC moves are already discussed the model section and

 doi:10.20944/preprints202208.0366.v1

the third, which models the exchange of triangles, provides the diffusive motion to different membrane components. Fig. 11 shows the two examples of the membrane budding due to multiple components on the membrane and both components are shown by two different colors. Since both component of the membrane have zero spontaneous curvature (Fig. 11(a)), budding is driven by the line tension of the domain boundary. In the another example shown in Fig. 11b, budding in the multicomponent membranes is induced due to one component having zero spontaneous curvature and another with nonzero curvature.

V. CHALLENGES AND WAY FORWARD IN THE MESOSCOPIC "MECHANICS" BASED METHODS IN MEMBRANE REMODELING

One of the fundamental assumption in the mechanics based mesoscopic method in the field of membrane curvature and remodeling is the representation of membrane as thin uniform elastic sheet. The constitutive equations, the guiding Hamiltonian and assumptions on material properties of the membrane are hugely simplified and efforts needs to be made to enhance the membrane representation that accounts for asymmetry across leaflets and heterogeneity in the lateral organization besides other features. Also, since most of these systems are stabilized far away from equilibrium, the mesoscopic modeling needs to be more "active" (non-equilibrium based) in nature and framework needs to be developed and evolved in that direction. Advancements made in this area by theoretical biophysicists with their advance theories and phenomenological models[165–170] need to be translated to multiscale modeling work with chemical specificity. Recently, more than 20 experts in the membrane remodeling area from around the world came together and wrote a beautiful topical review as a collection of short papers titled "The 2018 biomembrane curvature and remodeling road map"[171], which lays down a manifesto for future explorations in the field. Here, in this review, we focus on how mesoscopic modeling, which is largely based on analytical theories with parsimonious number of Physics based parameters, can be improved to more closely capture the chemical complexity and diversity of the biological components as well as incorporate both passive and active interactions that drive these processes.

Preprints (www.preprints.org) | NOT PEER-REVIEWED | Posted: 22 August 2022 doi:10.20944/preprints202208.0366.v1

A. Molecular reconstruction: Capturing the chemical diversity using back mapping

Plasma membrane is made up of more than 800 lipids types and recent lipidomics data suggest that there are more than 35,000 different lipids types in the eukaryotic cells[155–157,172–174]. The heterogeneity in membrane is quite well established - both in terms of lateral organization on the surface due to the variety of lipids present as well as the asymmetry across leaflets that manifest in features such as local line tensions around domain boundaries, spontaneous curvature, differential stress and bending modulus to name a few. Ideally, high-resolution all-atom molecular dynamics (AAMD) simulation is the most preferred method to faithfully recapitulate the huge molecular diversity of the membrane-remodeling system but infeasible due to the computational costs. For emergent process such as ones described above, even highly coarse-grained molecular dynamics (CGMD) models are computationally prohibitive since some of the processes takes places in seconds and minutes timescales. One of the ways to circumvent the problem is to connect the multiple length and times scales by a combination of continuum-level mesoscopic modeling and coarse-grained molecular simulations guided by experimental inputs both at the imaging level as well as at structural and biochemical scales. The approach would allow us to study both the general physical principles and investigate the molecular-level chemical specificity behind the membrane remodelling.

One of the first attempt in reconstructing particle representation from continuum and/or imaging data was made in Voth group where they used "inverse coarse-graining" for rebuilding a higher resolution model from a lower resolution model and found that this approach leads to the stability of structures in CG simulation[175]. Of late, with rising computational powers and with better coarse-grained model, the back mapping has become a focus area and is quite achievable with minimal ambiguity. In that regard, recent work published in from Siewert Marrink's group is worth noticing and has set the stage for further progress in this field[176]. Using the reconstructed CGMD simulations, we could explore how the chemical specificity and molecular interactions at residues and lipid level propagate to physical scales and vice-versa. With this kind of framework, physical properties such as membrane bending modulus, protein curvatures, protein-protein interactions strength and other larger scale properties can be connected to molecular scales and allow us to see how changes in

 doi:10.20944/preprints202208.0366.v1

molecular interactions leads to larger scales effects such as nature of proteins aggregates and deformation profile.

B. Cytoskeleton-mediated membrane reshaping: Going beyond passive scaffold-based modeling

Along with the scaffold proteins, a heavier investment needs to be made by modellers towards the role of cytoskeleton while studying membrane deformation using mechanics models. The biochemical pathways that trigger cell deformations such as filopodia and endocytic buds are regulated by the underlying actin network. Experiments have convincingly shown that actin filament dynamics and its assembly into a growing network of meshwork are the primary modulators of formation and maintenance of actin-rich filopodia and endocytic buds. The complex machinery involving multiple adaptor and kinase proteins such as Arp2/3 and VASP tightly regulate the branching and growth of actin filaments, which in turn pushes or pulls on the membrane leading to membrane protrusion or invaginations. In order to elucidate the physical mechanisms underlying the cytoskeleton-mediated membrane deformation, any modeling approach must account for physical contact between the membrane and the actin filament and its meshwork as well account for the force exerted by the growing actin network at the surface of the membrane[177,178].

The DTS framework provides an opportunity to study such systems that can be put under the category of "confined/growing" filaments in soft vesicle. Recently, the DTS framework was enhanced by Anirban Sain and co-workers to explore the effect of long semi-rigid haemoglobin protein filaments inside the the red blood cell (RBC) to unravel the factors leading to pathologically debilitating deformation of RBCs in sickle cell anemia[98]. While the membrane was represented in the usual manner as a closed dynamically-triangulated network, the authors made use of a worm-like chain model for the hemoglobin filament. Using these two constructs in the continuum mechanics Hamiltonian based framework, they explored the equilibrium configuration of the filament- vesicle hybrid system. Besides the oft-studied effects of membrane modulus and filament rigidities on the equilibrium shape of outer membrane (RBC in this case), the model is also capable of studying the effect of 3D confinement of the helical filament conformations and can explore the dynamics between

 doi:10.20944/preprints202208.0366.v1

the surface area versus volume of confining membrane – features that seem to have important relevance to plasma membrane deformation due to fibrous proteins such as f-actin and microtubules.

 doi:10.20944/preprints202208.0366.v1

VI. AUTHOR CONTRIBUTIONS

AS created the blue prints for the review with the help of GK. GK wrote the paper with help from AS and SCD.

VII. ACKNOWLEDGMENTS

GK would like to acknowledge financial support from DST India, DBT-IISc and SERB. High-performance computing facility "Beagle" setup from grants by a partnership between the Department of Biotechnology of India and the Indian Institute of Science (IISc-DBT partnership progra) are greatly acknowledged. A.S. is thankful for the early career grant from DST, India. A.S. also thanks the DST for the National Supercomputing Mission grant. FIST program sponsored by the Department of Science and Technology and UGC, Centre for Advanced Studies and Ministry of Human Resource Development, India is gratefully acknowledged by the authors. This research was also supported in part by the National Science Foundation under Grant No. NSF PHY-1748958 (KITP e-visit).

VIII. COMPLIANCE WITH ETHICAL STANDARDS

Funding: This study is funded by the DST under the National Supercomputing Mission grant $DST/NSM/RD-HPC-Applications/2021/03.10$. This research was also supported in part by the National Science Foundation under Grant No. NSF PHY-1748958 (KITP e-visit). GK is supported as a National Postdoctoral fellow by SERB and SCD thanks the MoE for his financial support.

Conflict of Interest: Author GK declares that he has no conflict of interest. Author SCD declares that he has no conflict of interest. Author AS declares that he has no conflict of interest.

Ethical approval: This article does not contain any studies with human participants or animals performed by any of the authors.

REFERENCES

[1]Michael M. Kozlov and Justin W. Taraska. Generation of nanoscopic membrane curvature for membrane trafficking. Nature reviews Molecular cell biology, 2022.

[2]Marko Kaksonen and Aurélien Roux. Mechanisms of clathrin-mediated endocytosis. Nature reviews Molecular cell biology, 19(5):313–326, 2018.

[3]Kohji Takei, Vladimir I Slepnev, Volker Haucke, and Pietro De Camilli. Functional partnership between amphiphysin and dynamin in clathrin-mediated endocytosis. Nature cell biology, 1(1):33–39, 1999.

[4]Jennifer Lippincott-Schwartz. Cytoskeletal proteins and golgi dynamics. Current Opinion in Cell Biology, 10(1):52–59, 1998.

[5]Songyu Wang, Hanna Tukachinsky, Fabian B Romano, and Tom A Rapoport. Cooperation of the er-shaping proteins atlastin, lunapark, and reticulons to generate a tubular membrane network. eLife, 5:e18605, sep 2016.

[6]Jez Carlton, Miriam Bujny, Anna Rutherford, and Pete Cullen. Sorting nexins – unifying trends and new perspectives. Traffic, 6(2):75–82, 2005.

[7]M. Sharma and S. Caplan. BAR Domains and BAR Domain Superfamily Proteins, volume 2, pages 491–502. 2016.

[8]Michal Skruzny, Ambroise Desfosses, Simone Prinz, Svetlana O Dodonova, Anna Gieras, Charlotte Uetrecht, Arjen J Jakobi, Marc Abella, Wim JH Hagen, Joachim Schulz, et al. An organized co-assembly of clathrin adaptors is essential for endocytosis. Developmental Cell, 33(2):150–162, 2015.

[9]Adam Frost, Rushika Perera, Aurélien Roux, Krasimir Spasov, Olivier Destaing, Edward H Egelman, Pietro De Camilli, and Vinzenz M Unger. Structural basis of membrane invagination by f-bar domains. Cell, 132(5):807–817, 2008.

[10]Guillaume Drin and Bruno Antonny. Amphipathic helices and membrane curvature. FEBS letters, 584(9):1840–1847, 2010.

[11]Diego A Ramirez-Diaz, Adrián Merino-Salomón, Fabian Meyer, Michael Heymann, Germán Rivas, Marc Bramkamp, and Petra Schwille. Ftsz induces membrane deformations via torsional stress upon gtp hydrolysis. Nature communications, 12(1):1–11, 2021.

[12]Toshiki Itoh, Kai S Erdmann, Aurelien Roux, Bianca Habermann, Hauke Werner, and Pietro De Camilli. Dynamin and the actin cytoskeleton cooperatively regulate plasma membrane invagination by bar and f-bar proteins. Developmental cell, 9(6):791–804, 2005.

[13]Zheng Shi. Mechanisms of membrane remodeling by peripheral proteins and divalent cations. PhD thesis, University of Pennsylvania, University of Pennsylvania, 2015.

[14]Judith Klumperman and Thomas Pucadyil. Understanding membrane traffic from molecular ensemble, energetics, and the cell biology of participant components. Current Opinion in Cell Biology, 71, 07 2021.

[15]Andrej Sali. From integrative structural biology to cell biology. Journal of Biological Chemistry, 296:100743, 2021.

[16]Shruthi Viswanath and Andrej Sali. Optimizing model representation for integrative structure determination of macromolecular assemblies. Proceedings of the National Academy of Sciences, 116(2):540–545, 2019.

[17]Alexander J Pak and Gregory A Voth. Advances in coarse-grained modeling of macromolecular complexes. Current Opinion in Structural Biology, 52:119–126, 2018. Cryo electron microscopy: the impact of the cryo-EM revolution in biology • Biophysical and computational methods - Part A.

[18]Daniel Russel, Keren Lasker, Ben Webb, Javier Velázquez-Muriel, Elina Tjioe, Dina Schneidman-Duhovny, Bret Peterson, and Andrej Sali. Putting the pieces together: Integrative modeling platform software for structure determination of macromolecular assemblies. PLOS Biology, 10(1):1–5, 01 2012.

[19]Henry Van Den Bedem and James S Fraser. Integrative, dynamic structural biology at atomic resolution—it's about time. Nature methods, 12(4):307–318, 2015.

[20]Massimiliano Bonomi, Carlo Camilloni, Andrea Cavalli, and Michele Vendruscolo. Metainference: A bayesian inference method for heterogeneous systems. Science Advances, 2(1):e1501177, 2016.

[21]Wouter Boomsma, Jesper Ferkinghoff-Borg, and Kresten Lindorff-Larsen. Combining experiments and simulations using the maximum entropy principle. PLOS Computational Biology, 10(2):1–9, 02 2014.

[22]D. M. Deaven and K. M. Ho. Molecular geometry optimization with a genetic algorithm. Phys. Rev. Lett., 75:288–291, Jul 1995.

[23]Philip D Blood and Gregory A Voth. Direct observation of bin/amphiphysin/rvs (bar) domain-induced membrane curvature by means of molecular dynamics simulations. Proceedings of the National Academy of Sciences, 103(41):15068–15072, 2006.

[24]Weria Pezeshkian, Allan Grønhøj Hansen, Ludger Johannes, Himanshu Khandelia, Julian C Shillcock, PB Sunil Kumar, and John Hjort Ipsen. Membrane invagination induced by shiga toxin b-subunit: from molecular structure to tube formation. Soft matter, 12(23):5164–5171, 2016.

[25]Molecular modeling of lipid membrane curvature induction by a peptide: More than simply shape. Biophysical Journal, 106(9):1958–1969, 2014.

[26]Juan Perilla and Klaus Schulten. Physical properties of the hiv-1 capsid from all-atom molecular dynamics simulations. Nature Communications, 8:15959, 07 2017.

[27]Mijo Simunovic, Anand Srivastava, and Gregory A. Voth. Linear aggregation of proteins on the membrane as a prelude to membrane remodeling. Proceedings of the National Academy of Sciences, 110:20396 – 20401, 2013.

[28]Benedict Reynwar, Gregoria Illya, V. Harmandaris, Martin Müller, Kurt Kremer, and Markus Deserno. Aggregation and vesiculation of membrane proteins by curvature-mediated interactions. Nature, 447:461–464, 05 2007.

[29]Ryan P Bradley and Ravi Radhakrishnan. Curvature–undulation coupling as a basis for curvature sensing and generation in bilayer membranes. Proceedings of the National Academy of Sciences, 113(35):E5117–E5124, 2016.

[30]Alexander J. Pak, John M. A. Grime, Prabuddha Sengupta, Antony K. Chen, Aleksander E. P. Durumeric, Anand Srivastava, Mark Yeager, John A. G. Briggs, Jennifer Lippincott-Schwartz, and Gregory A. Voth. Immature hiv-1 lattice assembly dynamics are regulated by scaffolding from nucleic acid and the plasma membrane. Proceedings of the National Academy of Sciences, 114(47):E10056–E10065, 2017.

[31]John Grime, James Dama, Barbie Ganser-Pornillos, Cora Woodward, Grant Jensen, Mark Yeager, and Gregory Voth. Coarse-grained simulation reveals key features of hiv-1 capsid self-assembly. Nature communications, 7:11568, 05 2016.

[32]M. E. Johnson, A. Chen, J. R. Faeder, P. Henning, I. I. Moraru, M. Meier-Schellersheim, R. F. Murphy, T. Prüstel, J. A. Theriot, and A. M. Uhrmacher. Quantifying the roles of space and stochasticity in computer simulations for cell biology and cellular biochemistry.

Molecular Biology of the Cell, 32(2):186–210, 2021.

[33]Peter B Canham. The minimum energy of bending as a possible explanation of the biconcave shape of the human red blood cell. Journal of theoretical biology, 26(1):61–81, 1970.

[34]Wolfgang Helfrich. Elastic properties of lipid bilayers: theory and possible experiments. Zeitschrift für Naturforschung c, 28(11-12):693–703, 1973.

[35]Thomas M Fischer. Bending stiffness of lipid bilayers. i. bilayer couple or single-layer bending? Biophysical journal, 63(5):1328–1335, 1992.

[36]Thomas M Fischer. Bending stiffness of lipid bilayers. ii. spontaneous curvature of the monolayers. Journal de Physique II, 2(3):327–336, 1992.

[37]Thomas M Fischer. Bending stiffness of lipid bilayers. iii. gaussian curvature. Journal de Physique II, 2(3):337–343, 1992.

[38]Thomas M Fischer. Bending stiffness of lipid bilayers: Iv. interpretation of red cell shape change. Biophysical journal, 65(2):687–692, 1993.

[39]Thoms M Fischer. Bending stiffness of lipid bilayers. v. comparison of two formulations. Journal de Physique II, 3(12):1795–1805, 1993.

[40]Udo Seifert, Karin Berndl, and Reinhard Lipowsky. Shape transformations of vesicles: Phase diagram for spontaneous-curvature and bilayer-coupling models. Physical review A, 44(2):1182, 1991.

[41]Udo Seifert. Configurations of fluid membranes and vesicles. Advances in physics, 46(1):13–137, 1997.

[42]Udo Seifert and Reinhard Lipowsky. Adhesion of vesicles. Physical Review A, 42(8):4768, 1990.

[43]Reinhard Lipowsky. The conformation of membranes. Nature, 349(6309):475–481, 1991.

[44]R Lipowsky. Bending of membranes by anchored polymers. EPL (Europhysics Letters), 30(4):197, 1995.

[45]R Lipowsky and E Sackmann. Structure and dynamics of membranes—from cells to vesicles (handbook of biological physics vol 1), 1995.

[46]Biswajit Gorai, Anil Kumar Sahoo, Anand Srivastava, Narendra M. Dixit, and Prabal K. Maiti. Concerted interactions between multiple gp41 trimers and the target cell lipidome may be required for hiv-1 entry. Journal of Chemical Information and Modeling,

61(1):444–454, 2021.

[47]Krishnakanth Baratam, Kirtika Jha, and Anand Srivastava. Flexible pivoting of dynamin pleckstrin homology domain catalyzes fission: insights into molecular degrees of freedom. Molecular Biology of the Cell, 32(14):1306–1319, 2021.

[48]Lena Harker-Kirschneck, Anne E Hafner, Tina Yao, Christian Vanhille-Campos, Xiuyun Jiang, Andre Pulschen, Fredrik Hurtig, Dawid Hryniuk, Siân Culley, Ricardo Henriques, et al. Physical mechanisms of escrt-iii–driven cell division. Proceedings of the National Academy of Sciences, 119(1):e2107763119, 2022.

[49]Pep Espanol and Patrick Warren. Statistical mechanics of dissipative particle dynamics. EPL (Europhysics Letters), 30(4):191, 1995.

[50]Robert D Groot and Patrick B Warren. Dissipative particle dynamics: Bridging the gap between atomistic and mesoscopic simulation. The Journal of chemical physics, 107(11):4423–4435, 1997.

[51]Robert D Groot and KL Rabone. Mesoscopic simulation of cell membrane damage, morphology change and rupture by nonionic surfactants. Biophysical journal, 81(2):725–736, 2001.

[52]Hiroshi Noguchi and Masako Takasu. Adhesion of nanoparticles to vesicles: A brownian dynamics simulation. Biophysical journal, 83:299–308, 08 2002.

[53]Marc Fuhrmans and Marcus Müller. Coarse-grained simulation of dynamin-mediated fission. Soft Matter, 11:1464–1480, 2015.

[54]Andela Šarić and Angelo Cacciuto. Fluid membranes can drive linear aggregation of adsorbed spherical nanoparticles. Phys. Rev. Lett., 108:118101, Mar 2012.

[55]Hakhamanesh Mostafavi, Sathish Thiyagarajan, Benjamin S. Stratton, Erdem Karatekin, Jason M. Warner, James E. Rothman, and Ben O'Shaughnessy. Entropic forces drive self-organization and membrane fusion by snare proteins. Proceedings of the National Academy of Sciences, 114(21):5455–5460, 2017.

[56]Adip Jhaveri, Dhruw Maisuria, Matthew Varga, Dariush Mohammadyani, and Margaret E Johnson. Thermodynamics and free energy landscape of bar-domain dimerization from molecular simulations. The Journal of Physical Chemistry B, 125(15):3739–3751, 2021.

[57]Gary S. Ayton and Gregory A. Voth. Multiscale simulation of protein mediated membrane remodeling. Seminars in Cell Developmental Biology, 21(4):357–362, 2010.

[58]Marissa G. Saunders and Gregory A. Voth. Coarse-graining methods for computational biology. Annual Review of Biophysics, 42(1):73–93, 2013.

[59]Sebastian Kmiecik, Dominik Gront, Michal Kolinski, Lukasz Wieteska, Aleksandra Elzbieta Dawid, and Andrzej Kolinski. Coarse-grained protein models and their applications. Chemical Reviews, 116(14):7898–7936, 2016.

[60]Mohsen Sadeghi, Thomas R. Weikl, and Frank Noé. Particle-based membrane model for mesoscopic simulation of cellular dynamics. The Journal of Chemical Physics, 148(4):044901, 2018.

[61]Alexander J Pak and Gregory A Voth. Advances in coarse-grained modeling of macromolecular complexes. Current Opinion in Structural Biology, 52:119–126, 2018.

[62]Mijo Simunovic, Patricia Bassereau, and Gregory A Voth. Organizing membrane-curving proteins: the emerging dynamical picture. Current Opinion in Structural Biology, 51:99–105, 2018.

[63]Weria Pezeshkian, Melanie König, Siewert J. Marrink, and John H. Ipsen. A multi-scale approach to membrane remodeling processes. Frontiers in Molecular Biosciences, 6, 2019.

[64]Weria Pezeshkian and Siewert J. Marrink. Simulating realistic membrane shapes. Current Opinion in Cell Biology, 71:103–111, 2021.

[65]John F. Presley, Carolyn Smith, Koty Hirschberg, Chad Miller, Nelson B. Cole, Kristien J. M. Zaal, and Jennifer Lippincott-Schwartz. Golgi membrane dynamics. Molecular Biology of the Cell, 9(7):1617–1626, 1998.

[66]Gia Voeltz, Melissa Rolls, and Tom Rapoport. Structural organization of the endoplasmic reticulum. EMBO reports, 3:944–50, 11 2002.

[67]Pierre Sens and Madan Rao. (re)modeling the golgi. Methods in cell biology, 118:299–310, 12 2013.

[68]Michael Nguyen, Yuqing Qiu, and Suriyanarayanan Vaikuntanathan. Organization and self-assembly away from equilibrium: Toward thermodynamic design principles. Annual Review of Condensed Matter Physics, 12:273–290, 03 2021.

[69]Amirali Hossein and Markus Deserno. Spontaneous curvature, differential stress, and bending modulus of asymmetric lipid membranes. Biophysical Journal, 118(3):624–642, 2020.

[70]Grace Brannigan and Frank L.H. Brown. A consistent model for thermal fluctuations and

protein-induced deformations in lipid bilayers. Biophysical Journal.

[71]Frank L.H. Brown. Elastic modeling of biomembranes and lipid bilayers. Annual Review of Physical Chemistry, 59(1):685–712, 2008.

[72]Frank L. H. Brown. Continuum simulations of biomembrane dynamics and the importance of hydrodynamic effects. Quarterly Reviews of Biophysics, 44(4):391–432, 2011.

[73]Hiroshi Noguchi. Acceleration and suppression of banana-shaped-protein-induced tubulation by addition of small membrane inclusions of isotropic spontaneous curvatures. Soft Matter, 13(42):7771–7779, 2017.

[74]Hiroshi Noguchi and Jean-Baptiste Fournier. Membrane structure formation induced by two types of banana-shaped proteins. Soft Matter, 13:4099–4111, 2017.

[75]Hiroshi Noguchi. Vesicle budding induced by binding of curvature-inducing proteins. Phys. Rev. E, 104:014410, Jul 2021.

[76]Amir Houshang Bahrami, Reinhard Lipowsky, and Thomas R Weikl. Tubulation and aggregation of spherical nanoparticles adsorbed on vesicles. Physical review letters, 109(18):188102, 2012.

[77]Amir H Bahrami, Michael Raatz, Jaime Agudo-Canalejo, Raphael Michel, Emily M Curtis, Carol K Hall, Michael Gradzielski, Reinhard Lipowsky, and Thomas R Weikl. Wrapping of nanoparticles by membranes. Advances in colloid and interface science, 208:214–224, 2014.

[78]Francesco Bonazzi, Carol K. Hall, and Thomas R. Weikl. Membrane morphologies induced by mixtures of arc-shaped particles with opposite curvature. Soft Matter, 17:268–275, 2021.

[79]Francesco Bonazzi and Thomas R. Weikl. Membrane morphologies induced by arc-shaped scaffolds are determined by arc angle and coverage. Biophysical Journal, 116(7):1239–1247, 2019.

[80]Hiroshi Noguchi and Jean-Baptiste Fournier. Membrane structure formation induced by two types of banana-shaped proteins. Soft Matter, 13(22):4099–4111, 2017.

[81]J Liam McWhirter, Gary Ayton, and Gregory A Voth. Coupling field theory with mesoscopic dynamical simulations of multicomponent lipid bilayers. Biophysical Journal, 87(5):3242–3263, 2004.

[82]Gary Ayton, J McWhirter, and Gregory Voth. A second generation mesoscopic lipid

bilayer model: Connections to field-theory descriptions of membranes and nonlocal hydrodynamics. The Journal of chemical physics, 124:64906, 03 2006.

[83]Wm G Hoover and CG Hoover. Links between microscopic and macroscopic fluid mechanics. Molecular Physics, 101(11):1559–1573, 2003.

[84]William Graham Hoover. Smooth particle applied mechanics: the state of the art. World Scientific, 2006.

[85]Aram Davtyan, Mijo Simunovic, and Gregory A Voth. The mesoscopic membrane with proteins (mesm-p) model. The Journal of Chemical Physics, 147(4):044101, 2017.

[86]Yacov Kantor and David R Nelson. Phase transitions in flexible polymeric surfaces. Physical Review A, 36(8):4020, 1987.

[87]A Baumgärtner and J-S Ho. Crumpling of fluid vesicles. Physical Review A, 41(10):5747, 1990.

[88]J-S Ho and A Baumgärtner. Simulations of fluid self-avoiding membranes. EPL (Europhysics Letters), 12(4):295, 1990.

[89]DM Kroll and Gerhard Gompper. The conformation of fluid membranes: Monte carlo simulations. Science, 255(5047):968–971, 1992.

[90]DM Kroll and Gerhard Gompper. Scaling behavior of randomly triangulated self-avoiding surfaces. Physical Review A, 46(6):3119, 1992.

[91]G Gompper and DM Kroll. Phase diagram and scaling behavior of fluid vesicles. Physical Review E, 51(1):514, 1995.

[92]G Gompper and DM Kroll. Triangulated-surface models of fluctuating membranes. Statistical mechanics of membranes and surfaces, pages 359–426, 2004.

[93]N. Ramakrishnan, P. B. Sunil Kumar, and John H. Ipsen. Monte carlo simulations of fluid vesicles with in-plane orientational ordering. Phys. Rev. E, 81:041922, Apr 2010.

[94]N. Ramakrishnan, P. B. Sunil Kumar, and John H. Ipsen. Modeling anisotropic elasticity of fluid membranes. Macromolecular Theory and Simulations, 20(7):446–450, 2011.

[95]N Ramakrishnan, John H Ipsen, and PB Sunil Kumar. Role of disclinations in determining the morphology of deformable fluid interfaces. Soft Matter, 8(11):3058–3061, 2012.

[96]K K Sreeja, John H Ipsen, and P B Sunil Kumar. Monte carlo simulations of fluid vesicles. Journal of Physics: Condensed Matter, 27(27):273104, jun 2015.

[97]Gaurav Kumar, N Ramakrishnan, and Anirban Sain. Tubulation pattern of membrane

vesicles coated with biofilaments. Physical Review E, 99(2):022414, 2019.

[98]Arabinda Behera, Gaurav Kumar, and Anirban Sain. Confined filaments in soft vesicles–the case of sickle red blood cells. Soft matter, 16(2):421–427, 2020.

[99]Arabinda Behera, Gaurav Kumar, Sk Ashif Akram, and Anirban Sain. Deformation of membrane vesicles due to chiral surface proteins. Soft Matter, 17(34):7953–7962, 2021.

[100]N. Ramakrishnan, P.B. Sunil Kumar, and Ravi Radhakrishnan. Mesoscale computational studies of membrane bilayer remodeling by curvature-inducing proteins. Physics Reports, 543(1):1–60, 2014.

[101]N Ramakrishnan, Ryan P Bradley, Richard W Tourdot, and Ravi Radhakrishnan. Biophysics of membrane curvature remodeling at molecular and mesoscopic lengthscales. Journal of Physics: Condensed Matter, 30(27):273001, jun 2018.

[102]Paul A Lebwohl and Gordon Lasher. Nematic-liquid-crystal order—a monte carlo calculation. Physical Review A, 6(1):426, 1972.

[103]Gaurav Kumar and Anand Srivastava. Membrane remodeling due to mixture of multiple types of curvature proteins (in press, jctc). bioRxiv, 2022.

[104]Claude Itzykson and J-B Zuber. Two-dimensional conformal invariant theories on a torus. Nuclear Physics B, 275(4):580–616, 1986.

[105]Netasan Ramakrishnan, PB Sunil Kumar, and John H Ipsen. Monte carlo simulations of fluid vesicles with in-plane orientational ordering. Physical Review E, 81(4):041922, 2010.

[106]Masaki Osawa, David E Anderson, and Harold P Erickson. Curved ftsz protofilaments generate bending forces on liposome membranes. The EMBO journal, 28(22):3476–3484, 2009.

[107]Netasan Ramakrishnan, PB Sunil Kumar, and John H Ipsen. Modeling anisotropic elasticity of fluid membranes. Macromolecular theory and simulations, 20(7):446–450, 2011.

[108]TC Lubensky and Jacques Prost. Orientational order and vesicle shape. Journal de Physique II, 2(3):371–382, 1992.

[109]Camilla Raiborg and Harald Stenmark. The escrt machinery in endosomal sorting of ubiquitylated membrane proteins. Nature, 458:445–52, 04 2009.

[110]Bruno Antonny, Christopher Burd, Pietro De Camilli, Elizabeth Chen, Oliver Daumke, Katja Faelber, Marijn Ford, Vadim A Frolov, Adam Frost, Jenny E Hinshaw, Tom Kirchhausen, Michael M Kozlov, Martin Lenz, Harry H Low, Harvey McMahon, Christien

Merrifield, Thomas D Pollard, Phillip J Robinson, Aurélien Roux, and Sandra Schmid. Membrane fission by dynamin: what we know and what we need to know. The EMBO Journal, 35(21):2270–2284, 2016.

[111]Katja Faelber, Martin Held, Song Gao, York Posor, Volker Haucke, Frank Noé, and Oliver Daumke. Structural insights into dynamin-mediated membrane fission. Structure, 20(10):1621–1628, 2012.

[112]Arthur A. Melo, Thiemo Sprink, Jeffrey K. Noel, Elena Vázquez Sarandeses, Chris van Hoorn, Justus Loerke, Christian M. T. Spahn, and Oliver Daumke. Cryo-electron tomography reveals structural insights into the membrane binding and remodeling activity of dynamin-like ehds. bioRxiv, 2021.

[113]R.C. Sarasij, Satyajit Mayor, and Madan Rao. Chirality-induced budding: A raft-mediated mechanism for endocytosis and morphology of caveolae? Biophysical Journal, 92(9):3140–3158, 2007.

[114]Hiroshi Noguchi. Shape transition from elliptical to cylindrical membrane tubes induced by chiral crescent-shaped protein rods. Scientific Reports, 9, 08 2019.

[115]BW Van der Meer, G Vertogen, AJ Dekker, and JGJ Ypma. A molecular-statistical theory of the temperature-dependent pitch in cholesteric liquid crystals. The Journal of Chemical Physics, 65(10):3935–3943, 1976.

[116]JR van Weering, RB Sessions, C Traer, DP Kloer, VK Bhatia, D Stamou, SR Carlsson, JH Hurley, and PJ Cullen. In vitro snx-bar assembly reveals molecular details of distinct endosomal tubule formation. EMBO J, 31:4466–80, 2012.

[117]Shuliang Chen, Tanvi Desai, James A McNew, Patrick Gerard, Peter J Novick, and Susan Ferro-Novick. Lunapark stabilizes nascent three-way junctions in the endoplasmic reticulum. Proceedings of the National Academy of Sciences, 112(2):418–423, 2015.

[118]Shuliang Chen, Peter Novick, and Susan Ferro-Novick. Er network formation requires a balance of the dynamin-like gtpase sey1p and the lunapark family member lnp1p. Nature cell biology, 14(7):707–716, 2012.

[119]Brian J Peter, Helen M Kent, Ian G Mills, Yvonne Vallis, P Jonathan G Butler, Philip R Evans, and Harvey T McMahon. Bar domains as sensors of membrane curvature: the amphiphysin bar structure. Science, 303(5657):495–499, 2004.

[120]Jennifer L Gallop, Christine C Jao, Helen M Kent, P Jonathan G Butler, Philip R Evans,

Ralf Langen, and Harvey T McMahon. Mechanism of endophilin n-bar domain-mediated membrane curvature. The EMBO journal, 25(12):2898–2910, 2006.

[121]Adam Frost, Vinzenz M Unger, and Pietro De Camilli. The bar domain superfamily: membrane-molding macromolecules. Cell, 137(2):191–196, 2009.

[122]Michitaka Masuda and Naoki Mochizuki. Structural characteristics of bar domain superfamily to sculpt the membrane. In Seminars in cell & developmental biology, volume 21, pages 391–398. Elsevier, 2010.

[123]Mijo Simunovic, Emma Evergren, Andrew Callan-Jones, and Patricia Bassereau. Curving cells inside and out: roles of bar domain proteins in membrane shaping and its cellular implications. Annual review of cell and developmental biology, 35:111–129, 2019.

[124]Natasza E Ziółkowska, Lena Karotki, Michael Rehman, Juha T Huiskonen, and Tobias C Walther. Eisosome-driven plasma membrane organization is mediated by bar domains. Nature structural & molecular biology, 18(7):854–856, 2011.

[125]Pieta K Mattila, Anette Pykalainen, Juha Saarikangas, Ville O Paavilainen, Helena Vihinen, Eija Jokitalo, and Pekka Lappalainen. Missing-in-metastasis and irsp53 deform pi (4, 5) p2-rich membranes by an inverse bar domain–like mechanism. The Journal of cell biology, 176(7):953–964, 2007.

[126]Feng-Ching Tsai, J. Michael Henderson, Zack Jarin, Elena Kremneva, Yosuke Senju, Julien Pernier, Oleg Mikhajlov, John Manzi, Konstantin Kogan, Christophe Le Clainche, Gregory A. Voth, Pekka Lappalainen, and Patricia Bassereau. Activated i-bar irsp53 clustering controls the formation of vasp-actin-based membrane protrusions. bioRxiv, 2022.

[127]Thomas R. Weikl. Membrane-mediated cooperativity of proteins. Annual Review of Physical Chemistry, 69(1):521–539, 2018.

[128]Mijo Simunovic, Anand Srivastava, and Gregory A. Voth. Linear aggregation of proteins on the membrane as a prelude to membrane remodeling. Proceedings of the National Academy of Sciences, 110(51):20396–20401, 2013.

[129]Mijo Simunovic, Patricia Bassereau, and Gregory A Voth. Organizing membrane-curving proteins: the emerging dynamical picture. Current Opinion in Structural Biology, 51:99–105, 2018.

[130]Mijo Simunovic, Anela Šarić, J. Michael Henderson, Ka Yee C. Lee, and Gregory A. Voth.

Long-range organization of membrane-curving proteins. ACS Central Science, 3(12):1246–1253, 2017.

[131]BJ Reynwar, G Illya, VA Harmandaris, MM Müller, K Kremer, and M. Deserno. Aggregation and vesiculation of membrane proteins by curvature-mediated interactions. Nature, (447):461–464, 2007.

[132]Anne-Sophie Nicot, Anne Toussaint, Valérie Tosch, Christine Kretz, Carina Wallgren-Pettersson, Erik Iwarsson, Helen Kingston, Jean-Marie Garnier, Valérie Biancalana, Anders Oldfors, et al. Mutations in amphiphysin 2 (bin1) disrupt interaction with dynamin 2 and cause autosomal recessive centronuclear myopathy. Nature genetics, 39(9):1134–1139, 2007.

[133]Aram Davtyan, Mijo Simunovic, and Gregory A. Voth. The mesoscopic membrane with proteins (mesm-p) model. The Journal of Chemical Physics, 147(4):044101, 2017.

[134]Hiroshi Noguchi and Jean-Baptiste Fournier. Membrane structure formation induced by two types of banana-shaped proteins. Soft Matter, 13:4099–4111, 2017.

[135]Wade F Zeno, Upayan Baul, Wilton T Snead, Andre CM DeGroot, Liping Wang, Eileen M Lafer, D Thirumalai, and Jeanne C Stachowiak. Synergy between intrinsically disordered domains and structured proteins amplifies membrane curvature sensing. Nature communications, 9(1):1–14, 2018.

[136]David J Busch, Justin R Houser, Carl C Hayden, Michael B Sherman, Eileen M Lafer, and Jeanne C Stachowiak. Intrinsically disordered proteins drive membrane curvature. Nature communications, 6(1):1–11, 2015.

[137]Christoph Kalthoff, Jürgen Alves, Claus Urbanke, Ruth Knorr, and Ernst J Ungewickell. Unusual structural organization of the endocytic proteins ap180 and epsin 1. Journal of Biological Chemistry, 277(10):8209–8216, 2002.

[138]Raunaq Deo, Manish S Kushwah, Sukrut C. Kamerkar, Nagesh Y. Kadam, Srishti Dar, Kavita Babu, Anand Srivastava, and Thomas J. Pucadyil. Atp-dependent membrane remodeling links ehd1 functions to endocytic recycling. Nature Communications, 9, 2018.

[139]Soumya Bhattacharyya and Thomas J. Pucadyil. Cellular functions and intrinsic attributes of the atp-binding eps15 homology domain-containing proteins. Protein Science, 29(6):1321–1330, 2020.

[140]James Hofrichter, Philip D Ross, and William A Eaton. Kinetics and mechanism of deoxy-

hemoglobin s gelation: a new approach to understanding sickle cell disease. Proceedings of the National Academy of Sciences, 71(12):4864–4868, 1974.

[141]Noboru Mizushima, Tamotsu Yoshimori, and Yoshinori Ohsumi. The role of atg proteins in autophagosome formation. Annual review of cell and developmental biology, 27:107–132, 2011.

[142]Noboru Mizushima, Beth Levine, Ana Maria Cuervo, and Daniel J Klionsky. Autophagy fights disease through cellular self-digestion. nature, 451(7182):1069–1075, 2008.

[143]Shusaku T Shibutani and Tamotsu Yoshimori. A current perspective of autophagosome biogenesis. Cell research, 24(1):58–68, 2014.

[144]Robin Mathew, Vassiliki Karantza-Wadsworth, and Eileen White. Role of autophagy in cancer. Nature Reviews Cancer, 7(12):961–967, 2007.

[145]Joëlle Botti, Mojgan Djavaheri-Mergny, Yannick Pilatte, and Patrice Codogno. Autophagy signaling and the cogwheels of cancer. Autophagy, 2(2):67–73, 2006.

[146]Devrim Gozuacik and Adi Kimchi. Autophagy and cell death. Current topics in developmental biology, 78:217–245, 2007.

[147]Alfred J Meijer and Patrice Codogno. Signalling and autophagy regulation in health, aging and disease. Molecular aspects of medicine, 27(5-6):411–425, 2006.

[148]Amir Houshang Bahrami, Mary G Lin, Xuefeng Ren, James H Hurley, and Gerhard Hummer. Scaffolding the cup-shaped double membrane in autophagy. PLoS computational biology, 13(10):e1005817, 2017.

[149]Richard W Tourdot, N Ramakrishnan, and Ravi Radhakrishnan. Defining the free-energy landscape of curvature-inducing proteins on membrane bilayers. Physical Review E, 90(2):022717, 2014.

[150]Richard W Tourdot, N Ramakrishnan, Kshitiz Parihar, and Ravi Radhakrishnan. Quantification of curvature sensing behavior of curvature-inducing proteins on model wavy substrates. The Journal of Membrane Biology, pages 1–10, 2022.

[151]Jin Liu, Richard Tourdot, Vyas Ramanan, Neeraj J Agrawal, and Ravi Radhakrishanan. Mesoscale simulations of curvature-inducing protein partitioning on lipid bilayer membranes in the presence of mean curvature fields. Molecular physics, 110(11-12):1127–1137, 2012.

[152]Richard W Tourdot, N Ramakrishnan, Tobias Baumgart, and Ravi Radhakrishnan. Appli-

cation of a free-energy-landscape approach to study tension-dependent bilayer tubulation mediated by curvature-inducing proteins. Physical Review E, 92(4):042715, 2015.

[153]Luka Mesarec, Wojciech Góźdź, Samo Kralj, Miha Fošnarič, Samo Penič, Veronika Kralj-Iglič, and Aleš Iglič. On the role of external force of actin filaments in the formation of tubular protrusions of closed membrane shapes with anisotropic membrane components. European Biophysics Journal, 46(8):705–718, 2017.

[154]S Jonathan Singer and Garth L Nicolson. The fluid mosaic model of the structure of cell membranes: Cell membranes are viewed as two-dimensional solutions of oriented globular proteins and lipids. Science, 175(4023):720–731, 1972.

[155]Kui Yang and Xianlin Han. Lipidomics: techniques, applications, and outcomes related to biomedical sciences. Trends in biochemical sciences, 41(11):954–969, 2016.

[156]Andrej Shevchenko and Kai Simons. Lipidomics: coming to grips with lipid diversity. Nature reviews Molecular cell biology, 11(8):593, 2010.

[157]Britta Brügger. Lipidomics: analysis of the lipid composition of cells and subcellular organelles by electrospray ionization mass spectrometry. Annual review of biochemistry, 83:79–98, 2014.

[158]Oswald Quehenberger, Aaron M Armando, Alex H Brown, Stephen B Milne, David S Myers, Alfred H Merrill, Sibali Bandyopadhyay, Kristin N Jones, Samuel Kelly, Rebecca L Shaner, Cameron M, Elaine Wang, Robert C, Robert M, Thomas J, Christian RH, Ziqiang Guan, Gregory M, David A, Dawid W, Jeffery G, Shankar Subramaniam, Eoin Fahy, and Edward A. Lipidomics reveals a remarkable diversity of lipids in human plasma. Journal of lipid research, pages jlr–M009449, 2010.

[159]Kandice R Levental, Joseph H Lorent, Xubo Lin, Allison D Skinkle, Michal A Surma, Emily A Stockenbojer, Alemayehu A Gorfe, and Ilya Levental. Polyunsaturated lipids regulate membrane domain stability by tuning membrane order. Biophysical journal, 110(8):1800–1810, 2016.

[160]Matthew B Stone, Sarah A Shelby, and Sarah L Veatch. Super-resolution microscopy: Shedding light on the cellular plasma membrane. Chemical reviews, 117(11):7457–7477, 2017.

[161]PB Sunil Kumar, Gerhard Gompper, and Reinhard Lipowsky. Budding dynamics of multicomponent membranes. Physical review letters, 86(17):3911, 2001.

[162]Aleš Iglič, Blaž Babnik, Ulrike Gimsa, and Veronika Kralj-Iglič. On the role of membrane anisotropy in the beading transition of undulated tubular membrane structures. Journal of Physics A: Mathematical and General, 38(40):8527, 2005.

[163]Miha Fošnarič, Aleš Iglič, Tomaž Slivnik, and Veronika Kralj-Iglič. Flexible membrane inclusions and membrane inclusions induced by rigid globular proteins. Advances in planar lipid bilayers and liposomes, 7:143–168, 2008.

[164]Doron Kabaso, Nataliya Bobrovska, Wojciech Góźdź, Nir Gov, Veronika Kralj-Iglič, Peter Veranič, and Aleš Iglič. On the role of membrane anisotropy and bar proteins in the stability of tubular membrane structures. Journal of biomechanics, 45(2):231–238, 2012.

[165]Madan Rao and Satyajit Mayor. Active organization of membrane constituents in living cells. Current Opinion in Cell Biology, 29.

[166]Andre C. Barato and Udo Seifert. Thermodynamic uncertainty relation for biomolecular processes. Phys. Rev. Lett., 114:158101, Apr 2015.

[167]Michael Nguyen and Suriyanarayanan Vaikuntanathan. Design principles for nonequilibrium self-assembly. Proceedings of the National Academy of Sciences, 113(50):14231–14236, 2016.

[168]Arunkumar Bupathy, Daan Frenkel, and Srikanth Sastry. Temperature protocols to guide selective self-assembly of competing structures. Proceedings of the National Academy of Sciences, 119(8):e2119315119, 2022.

[169]Sriram Ramaswamy. The mechanics and statistics of active matter. Annual Review of Condensed Matter Physics, 1(1):323–345, 2010.

[170]M. C. Marchetti, J. F. Joanny, S. Ramaswamy, T. B. Liverpool, J. Prost, Madan Rao, and R. Aditi Simha. Hydrodynamics of soft active matter. Rev. Mod. Phys., 85:1143–1189, Jul 2013.

[171]Patricia Bassereau, Rui Jin, Tobias Baumgart, Markus Deserno, Rumiana Dimova, Vadim A Frolov, Pavel V Bashkirov, Helmut Grubmüller, Reinhard Jahn, H Jelger Risselada, Ludger Johannes, Michael M Kozlov, Reinhard Lipowsky, Thomas J Pucadyil, Wade F Zeno, Jeanne C Stachowiak, Dimitrios Stamou, Artù Breuer, Line Lauritsen, Camille Simon, Cécile Sykes, Gregory A Voth, and Thomas R Weikl. The 2018 biomembrane curvature and remodeling roadmap. Journal of Physics D: Applied Physics, 51(34):343001, 2018.

[172]William Dowhan. Understanding phospholipid function: Why are there so many lipids? Journal of Biological Chemistry, 292(26):10755–10766, 2017.

[173]Gerrit van Meer and Anton IPM de Kroon. Lipid map of the mammalian cell. J Cell Sci, 124(1):5–8, 2011.

[174]Sahithya S Iyer and Anand Srivastava. Degeneracy in molecular scale organization of biological membranes. Soft Matter, 16(29):6752–6764, 2020.

[175]Haosheng Cui, Edward Lyman, and Gregory A Voth. Mechanism of membrane curvature sensing by amphipathic helix containing proteins. Biophysical journal, 100(5):1271–1279, 2011.

[176]Weria Pezeshkian, Melanie König, Tsjerk A Wassenaar, and Siewert J Marrink. Backmapping triangulated surfaces to coarse-grained membrane models. Nature communications, 11(1):1–9, 2020.

[177]Cécile Sykes and Julie Plastino. Cell biology: Actin filaments up against a wall. , 464(7287):365–366, March 2010.

[178]Andrea Picco, Wanda Kukulski, Hetty E. Manenschijn, Tanja Specht, John A. G. Briggs, and Marko Kaksonen. The contributions of the actin machinery to endocytic membrane bending and vesicle formation. Molecular Biology of the Cell, 29(11):1346–1358, 2018.